Proyecto Singular; Desarrollo de una metodología para el diseño, control y optimización de sistemas naturales resilientes de depuración de bajo costo basados en tratamientos anaerobios.

Objetivo general del proyecto: Potenciar la investigación, el desarrollo tecnológico y la innovación a través de la creación de un clúster tecnológico que mitigue el cambio climático en el ciclo integral del agua, mediante tecnologías limpias e innovadoras internas y externas al ciclo

Actividad 2.1.2:	Identificación y análisis de los procesos y etapas en el ciclo del agua y sus particularidades en cada región.
Actividad 2.3.2:	Mitigación del cambio climático. Nexus CO2-Agua-Energía-Alimentos.
	Búsqueda de Fondos y sistemas de financiación para la implantación de los proyectos singulares.
Actividad 4:	Comunicación.

Fecha revisión	Autores:	Entidad	Versión	Anotaciones
01/09/2022	Saulo M. Brito	ULPGC		
	Alejandro Ramos	ULPGC		
	Carlos Mendieta	ULPGC		
	Sebastián O. Pérez	ULPGC		

Resumen ejecutivo

En este trabajo se desarrolla un marco teórico para el diseño de biodigestores anaerobios no convencionales tipo lagos, lagunas, estanques naturales y estanques artificiales, para el tratamiento de efluentes con alta carga orgánica procedente de granjas ganaderas. Esta propuesta que más allá de competir con las tecnologías que existen hoy en día, lo que pretende es aportar nuevas soluciones para su aplicación, de manera especial, en aquellas zonas rurales o granjas aisladas que tenga pocas posibilidades de acceder a las plantas de tratamiento de aguas centralizadas y a los sistemas generales de suministro de energía. El fundamento del proyecto singular se basa en la descripción del comportamiento de la biomasa, bacterias y archeas, que conforma el ecosistema bacteriano dentro de los digestore anaerobios. La singularidad de esta propuesta radica en las características del funcionamiento estos reactores, ya que se encuentran exento de sistemas de mezclado. La descripción del modelo se dificulta enormemente frente a la gran mayoría propuestos hasta la fecha, de parámetros concentrados, puesto que es necesario definir el comportamiento de los diferentes microorganismos que intervienen, en cada punto del espacio y en cada instante de tiempo. Se trata de un modelo de parámetros distribuidos. Con este tipo de solución se pretende desarrollar sistemas de tratamientos naturales de bajo coste, respetuoso con el medioambiente, resilientes, y con posibilidad de sumarse al modelo de economía circular.

ÍNDICE DE CONTENIDOS

1. introducción

El incremento de la producción de las explotaciones ganaderas intensivas en todo el mundo, acompañados de la mala gestión del estiércol/residuo generado, acrecienta el riesgo de contaminación medioambiental. Las disposiciones legales existentes en torno a la protección del medioambiente, cada vez más exigentes, ha suscitado la necesidad de encontrar soluciones al tratamiento de los residuos orgánicos que se originan principalmente en las granjas pecuarias. Los sistemas naturales de tratamiento de aguas residuales basados en procesos de Digestión Anaerobia(SDNA) se presenta como una de las alternativas más atractiva dentro de las tecnologías no convencionales. Estas son asequibles económicamente, fáciles de usar y presentan menos exigencias en cuanto a las labores de operación y mantenimiento.

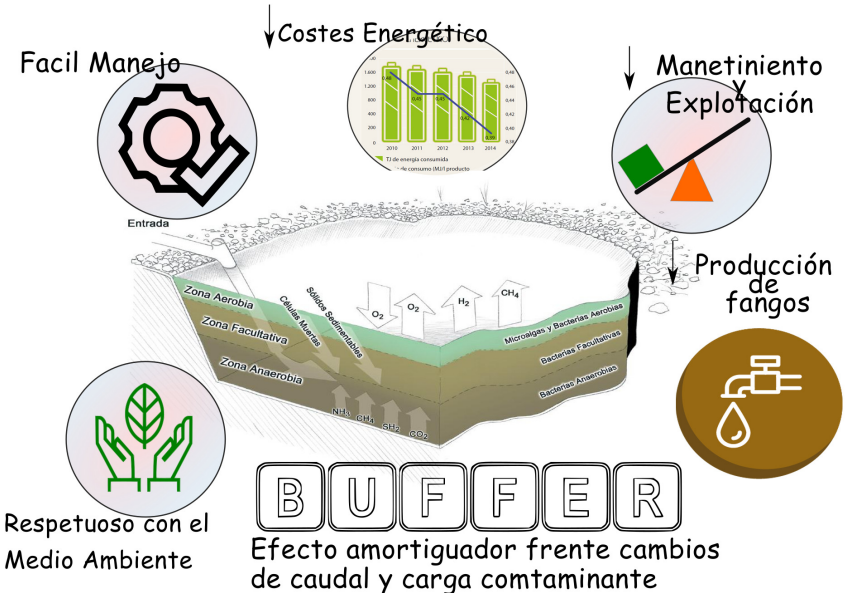

Figura 1: Ventajas de SDNA

El tratamiento anaerobio es una de las tecnologías más antiguas utilizadas para estabilizar residuos y aguas residuales. No obstante, es a partir de los años 80 cuando comienza a alcanzar un mayor interés gracias a los avances en la investigación sobre el funcionamiento de los procesos biológicos y bioquímicos que conforma la DA. Aunque su uso se vio limitado debido a una serie de factores relacionados, principalmente, con la necesidad de ocupar grandes superficies y consumir elevados tiempos de retención, en los últimos años se ha venido analizando nuevas oportunidades para la DA en el tratamiento de aguas, con una concepción más actual y que tiene que ver con la reducción de consumos energéticos, producción de lodos, emisiones a la atmósfera, etc.

Los primeros modelos que fueron planteados para sistemas de depuración natural eran modelos tipo caja negra que trataban de predecir su comportamiento sin importar lo que suceda en su interior durante todo el proceso. Aunque, algunos se diseñaban a partir de instalaciones que se encontraban ya en funcionamiento y en circunstancias similares, la gran mayoría empleaba modelos estadístico para la predicción. Hoy en día los modelos de Caja Negra siguen manteniéndose en la vanguardia, especialmente, aquellos que están

basados en redes neuronales artificiales. Otro tipo de modelos que se han venido desarrollando son los de tipo caja gris. En este caso, se combina modelos del conocimientos con modelos empíricos. Los modelos totalmente blancos o también llamados modelos de conocimiento, son el resultado de un exhaustivo y extenso modelado físico a partir de primeros principios. Este enfoque consiste en considerar todas las relaciones que existen entre las variables relevantes y utilizar un software como soporte para organizar dichas relaciones adecuadamente.

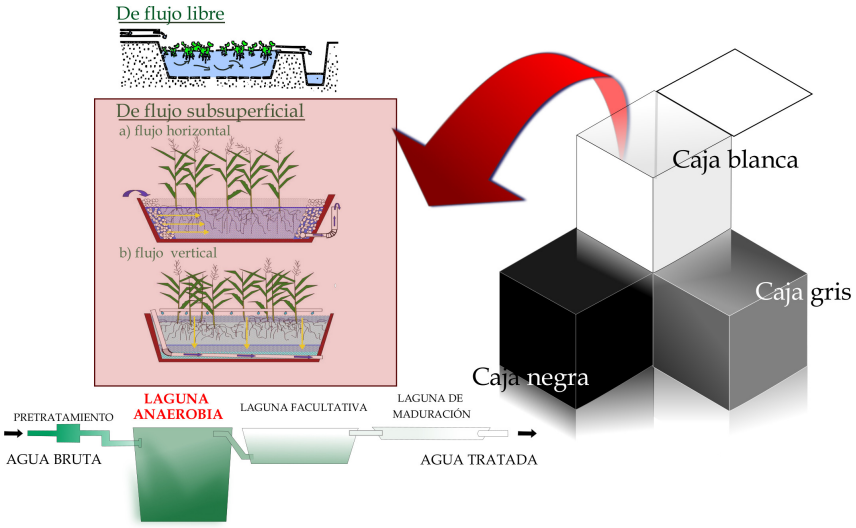

Figura 2: Clasificación de modelos en SDN. Los modelos de caja blanca, publicados, están referidos en su mayoría a los humedales artificiales de flujo subsuperficial

Hoy en día la gran mayoría de los modelos que se publican son de tipo Caja Negra o Caja Gris. Existe pocas publicaciones que proponen modelos tipo Caja Blanca, en especial, aquellos que están basados en procesos. De estos últimos, la gran mayoría han sido diseñados para humedales artificiales apoyándose en software comerciales para su diseño y resolución. En lo que respecta a los SDN basados en procesos de DA, la mayor parte de los estudios realizados están basados en modelos tipo caja negra o gris. Consecuentemente se hace necesario modelados dinámicos avanzados capaces de describir la evolución de las variables con el tiempo dentro de los SDN formados por por lagunas y estanques anaerobios.

La propuesta de este proyecto singular se fundamenta en la elaboración de una herramienta de cálculo, basada en la dinámica de fluidos computacional (CFD) para el diseño, el control y la optimización de sistemas naturales de depuración, y cuyo propósito es el de poder implementar tecnologías limpias e innovadoras capaces de producir energía a partir de procesos de DA. Se pretende, con el desarrollo de esta estrategia, que pueda ser materializada y personalizada en aquellas actividades pecuarias, en zonas rurales, y descentralizadas con el propósito de fomentar el desarrollo y la competitividad en materias de respeto al medio ambiente y la economía circular.

2. Objetivos

Desarrollo de un marco metodológico para SDN basado en estanques o lagunas anaerobias que permita el diseño de nuevas instalaciones y mejoras de las condiciones de funcionamiento de los sistemas ya existente para la eliminación de materia orgánica soluble, partículas y contaminantes microbiológicos. El único propósito de toda esta iniciativa

es el de mejorar el fortalecimiento de las relaciones existente entre cambio climático agua-energía-alimentos.

Para ello se pretende, con este proyecto singular, ir más allá de la clásica concepción convencional del término de las 3R[1] incorporando una visión mucho más global como podría ser la incorporación de ciertas unidades innovadoras en el sistema, diseño de lineas de flujos alternativas, o en la modificación del concepto global del enfoque para todo el tratamiento.

3. Oportunidad

Una de las opciones que ofrece los SDNA es que, además de utilizar los recursos locales en tecnologías de agua de baja energía y bajo carbono, tiene la capacidad de producir biogás. Este puede ser aprovechado posteriormente para la generación tanto de energía térmica y eléctrica, como biocombustible, adecuándose, de esta manera, al modelo de economía circular.

Este tipo de ingeniería basada en reactores sencillo, y dirigidos principalmente al sector ganadero de capacidad media o baja, que trata ofrecer energía y mejorar los problemas de contaminación, pretende competir con otros digestores de tipo convencional o incluso de alta eficiencia. Aunque a priori, estos últimos se presenta como solución idónea, ya que han sido diseñados para tal fin, su alto coste inicial y la complejidad del sistemas que hacen muy complicado su uso y mantenimiento, todo ello con el agravio que supone la dependencia energética y las consecuentes emisiones, producto de su funcionamiento, plantea la necesidad de buscar otro tipo de alternativas como es el caso de los SDNA.

Figura 3: Izda. Planta de biogas compuesta por digestores anaerobios termófilos a mezcla completa. Dcha. Sistemas de depuración natural formada por humedales, lagunas anaerobias y estanques de maduración

4. Planteamiento

Se aborda un serio problema medioambiental provocado por el incremento de las explotaciones ganaderas de tipo intensivas, que se encuentran localizadas de manera dispersa en el territorio, y que no pueden acceder a las redes municipales de alcantarillado público y depuración, ni tampoco a los sistemas de suministros de energía eléctrica. Teniendo en

[1]El concepto de las 3R contempla; 1. Reducir consumo energéticos, producción de lodos y emisiones a la atmósfera,.2 Rehusar lodos y aguas con calidad suficiente, 3. Recuperación de recursos, agua y energía en forma de biogas.

cuenta su contribución en las emisiones antropogénicas de gases de efecto invernadero, y centrándonos en dos aspectos muy actuales como son la energía y la contaminación, se trata de aplicar este tipo de tecnología en el ciclo del agua, de forma que pueda disminuirse tanto el consumo energético como los gases de efecto invernadero producido por dicha actividad.

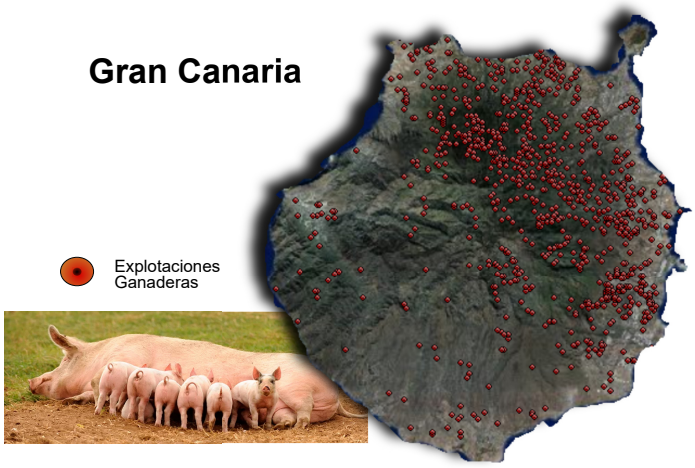

Figura 4: Mapa cartográfico de Gran Canaria donde figura los emplazamientos de todas las explotaciones ganaderas que han sido registradas en el Gobierno de Canarias

5. Destino de los resultado:

Se trata de un proyecto abierto a toda la comunidad investigadora, que a través de su difusión permita desarrollar futuros proyectos relacionado con el tratamiento de aguas, dentro del sector pecuario, y que puedan ser adaptados a las diferentes condiciones de una determinada región. Con ello es posible establecer comparativas frente a sistemas convencionales de depuración abordando aspectos como el análisis del ciclo de vida, huella de carbono, impacto y capacidad para la mitigación.

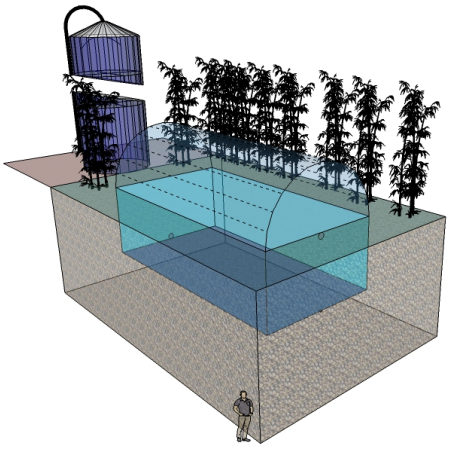

Figura 5: SDNA constituido por una laguna anaerobia, membrana de PVC y gasómetro

6. Beneficio medioambiental:

Control del producto y emisiones, reducción de contaminación y reducción del consumo energético en el sector a través de la producción de energía interna teniendo en cuenta la calidad y protección de las aguas.

7. Favorecimiento de la competitividad:

Basándose en la cultura de la innovación, así como de la lucha, mitigación y adaptación contra el cambio climático, y a través de la optimización energética y economía circular es posible obtener empresas sostenibles con un mayor índice de rentabilidad. Todo esto ayuda a visualizar el entorno rural como un lugar de oportunidades de empleo favoreciendo, de forma transversal, la lucha contra el despoblamiento rural.

8. Resultados previstos

1. Optimización de las tecnologías existentes en el tratamiento y depuración de aguas. Herramienta de apoyo/guía a la toma de decisiones para la planificación de estrategias de mitigación a partir de las tecnologías de depuración y regeneración de aguas.
2. Utilización de recursos locales en tecnologías de tratamiento de agua de baja energía y bajo carbono.
3. Integración directa energías renovables en las distintas etapas y procesos del ciclo del agua, por separado, o la sinergia entre varias.
4. Gestión de subproductos de tratamiento.
5. Incremento de la superficie regada con agua regenerada en las diferentes zonas.
6. Modelo de interacción entre las masas de agua de superficie y subterraneas en sistemas insulares.

9. Publicaciones

Este proyecto singular se ha materializado en las siguientes publicaciones;

TÍTULO: Application of a mathematical model to predict simultaneous reactions in anaerobic plug-flow reactors as a primary treatment for constructed wetlands. AUTORES (P.O.de firma): Saulo Manuel Brito Espino[1], Sebastián Ovidio Pérez Báez[1] , Alejandro Ramos Martín[2], Carlos Alberto Mendieta Pino[2].

REFERENCÍA-DOI: https://doi.org/10.1016/j.scitotenv.2019.136244, VOL. 713, PP 136244.

REVISTA: Science of the Total Environment

EDITORIAL: ELSEVIER

DESCRIPCIÓN CATEGORÍA	POSICIÓN:	Cuartil
ENVIRONMENTAL SCIENCES	25/274	Q1

LUGAR DE PUBLICACIÓN: NETHERLANDS
FECHA DE PUBLICACIÓN: ENERO 2020
F.I.: PUBLICADO (JCR-2020) → 7.9631

TÍTULO: A Framework Based on Finite Element Method (FEM) for Modelling and Assessing the Affection of the Local Thermal Weather Factors, on the Performance of Anaerobic Lagoons for the Natural Treatment of Swine Wastewater. AUTORES (P.O.de firma): Saulo Manuel Brito Espino[1], Sebastián Ovidio Pérez Báez[1] , Alejandro Ramos Martín[2], Carlos Alberto Mendieta Pino[2], Federico León Zerpa[2].
REFERENCÍA-DOI: https://doi.org/10.3390/w13070882, VOL. 13.
REVISTA: WATER
EDITORIAL: MDPI

DESCRIPCIÓN CATEGORÍA	POSICIÓN:	Cuartil
WATER RESOURCES	31/94	Q2

LUGAR DE PUBLICACIÓN: SWITZERLAND
FECHA DE PUBLICACIÓN: MARZO 2021
F.I.: PUBLICADO (JCR-2020) → 2.524

TÍTULO:Proposal of a Laboratory-Scale Anaerobic Biodigester for Introducing the Monitoring and Sensing Techniques, as a Potential Learning Tool in the Fields of Carbon Foot-Print Reduction and Climate Change Mitigation. AUTORES (P.O.de firma): Saulo Brito Espino[1], Federico León Zerpa[2], Jenifer Vaswani Reboso[1], Alejandro Ramos Martín[2], Carlos Alberto Mendieta Pino[1].
REFERENCÍA-DOI: https://doi.org/10.3390/w13172409.
REVISTA: WATER
EDITORIAL: MDPI **LUGAR DE PUBLICACIÓN:** SWITZERLAND

DESCRIPCIÓN CATEGORÍA	POSICIÓN:	Cuartil
WATER RESOURCES	31/94	Q2

FECHA DE PUBLICACIÓN: 1 septiembre 2021
F.I.: PUBLICADO (JCR-2020) → 2.524

Science of the Total Environment 713 (2020) 136244

Contents lists available at ScienceDirect

Science of the Total Environment

journal homepage: www.elsevier.com/locate/scitotenv

Application of a mathematical model to predict simultaneous reactions in anaerobic plug-flow reactors as a primary treatment for constructed wetlands

S. Brito-Espino [a,*], A. Ramos-Martín [b], S.O. Pérez-Báez [a], C. Mendieta-Pino [b]

[a] Institute for Environmental Studies and Natural Resources (i-UNAT) (ULPGC), Spain
[b] Department of Process Engineering, University of Las Palmas de Gran Canaria (ULPGC), Spain

HIGHLIGHTS

- A spatial and temporal mathematical model for anaerobic processes is proposed.
- Numerical methods and algorithms are useful mathematical tool for calculating PDEs.
- Simultaneous performances of twenty-one biochemical and physicochemical reactions occur.
- This flexible methodology permits the integration of various anaerobic phenomena.

GRAPHICAL ABSTRACT

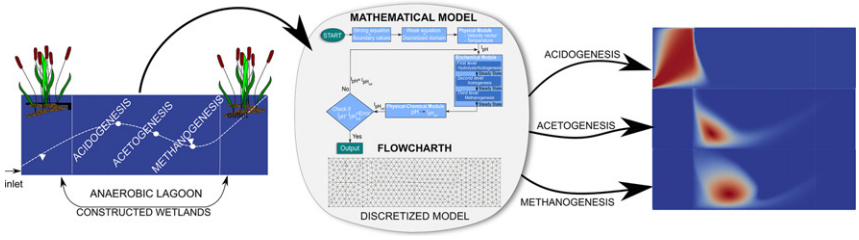

ARTICLE INFO

Article history:
Received 11 July 2019
Received in revised form 15 November 2019
Accepted 18 December 2019
Available online 3 January 2020

Editor: Jan Vymazal

Keywords:
Anaerobic digestion
ADM1
Finite elements method
Advection-diffusion-reaction
Freefem++

ABSTRACT

Anaerobic digestion technologies offer a set of advantages when they are implemented as a primary treatment phase prior to the use of constructed wetland systems in low cost wastewater facilities. The aim of this study is to describe a model capable of reflecting the complex functioning of anaerobic lagoons, subject to continuous flux in the feed pipe, taking into account that physicochemical properties are subject to a concentration gradient and biochemical ones to simultaneous reactions which depend on each other. Based on both Stokes and advection-diffusion-reaction equations, the proposed model includes twenty-one variables to describe hydraulic, physical, biochemical and physicochemical characteristics that take place in different points of the system and at different moments of time. Drawn up by the International Water Association, the anaerobic digestion model ADM1 is included for the purpose of incorporating the anaerobic processes in the calculation. The finite element method was used to solve the nonlinear, second order partial differential equations of the model. The calculation strategy was designed using a flowchart. Using the open-source FreeFem++ software, a simulation of the mathematical model, in bi-dimensional space, is presented to demonstrate the dynamic behaviour of the proposed model. This yields essential information about the performance of the substrate, cells, and the biochemical reaction products in each of the points within the reactor. Simulations show the potential of this methodology to carry out studies of the behaviour of each of the variables contemplated in the model, as well as comparative studies of the various possible options. In addition, this methodology can be used to help modify the behaviour of the variables based on digester geometry and the boundary values the system is subject to. From the results, it can be concluded that the proposed methodology can be a useful tool for calculating and designing the aforementioned synergistic systems of anaerobic digester plug-flow reactors and constructed wetlands.

* Corresponding author.
E-mail address: saulo.brito101@alu.ulpgc.es (S. Brito-Espino).

https://doi.org/10.1016/j.scitotenv.2019.136244
0048-9697/

1. Introduction

Constructed wetlands (CWs) are today considered a low-cost and eco-friendly technology and an alternative to conventional wastewater treatment systems especially in developing countries (Sanchez-Ramos et al., 2017; Laitinen et al., 2017). Although they have been widely used to treat different types of wastewater, this kind of technology is not efficient enough when it is the only method employed (Hartl et al., 2019). The use of anaerobic plug-flow reactors (APFR) as a primary treatment and constructed wetlands as a secondary treatment (Fig. 1), besides significantly reducing the sludge surplus, allows a decrease in the surface area required for CWs and, consequently, a reduction in building costs of up to the cost of 40% (Comino et al., 2013). Similarly, the clogging phenomenon in CWs is delayed as the organic load and suspended solids load are reduced by an APFR primary treatment (de la Varga et al., 2015; Alvarez et al., 2008). With these APFR-generated characteristics it is possible to extend the life of CWs to over 10 years (Wu et al., 2015).

There has been considerable interest on the part of the European Union and its member states with respect to the potential benefits of anaerobic digestion as an effective biotechnological tool, with financial incentives even being offered to farmers who proceed with the installation of these systems (Union, 2008; Kythreotou et al., 2014). In many cases, when there are no conventional means available, wastewaters are treated naturally. Often, for example, livestock farms may be orographically isolated as commonly occurs in the Canary Islands (Spain) (Mendieta-Pino et al., 2019; Brito-Espino et al., 2019). There is therefore a need for an in-depth analysis of these natural processes to allow a greater understanding and knowledge of how they function in order to optimize their design and efficiency (Lauwers et al., 2013).

The efficiency of anaerobic systems varies considerably due to the complex nature of all the physical, chemical and biological processes which take place within them (Kumar and Zhao, 2011; Imfeld et al., 2009). The elimination of pollutants depends on a number of variables including, among others, the wastewater application rate, the organic loading rate, the hydrologic regime, the hydraulic retention time and the operational mode (batch or continuous mode) (Wang et al., 2017). All of these are determined by a set of boundary values established in the system. Furthermore, hydrodynamic dispersion, as it is the result of the combination of the diffusion of the solute and the spatial and/or temporal variations of the local displacement velocity is therefore dependent on the type of flow, the geometry of the medium and the properties of the fluids (Rossi et al., 2017). The need to understand all these simultaneously occurring properties whose variables are closely interrelated requires the development of mathematical models that allow the internal workings of anaerobic digestion to be described (Donoso-Bravo et al., 2018).

Studies on anaerobic digestion have considered three different methodologies - 1. black-box models, in which, only the relationship between of the input and output variables is taken into account (Hu et al., 2018) - 2. grey-box models, mechanistic models in which the parameters have a physical interpretation but are adjustable (Lauwers et al., 2013) -3. white-box models, based on fundamental principles and a thorough knowledge of the underlying physical and chemical processes (Regmi et al., 2019).

Numerous white-box models have been developed since the 1970s. However as these models are limited in their design to a specific substrate or a small number of substrates with very similar compositions, they are not suitable for general use (Ivanovs et al., 2018). The anaerobic digester model No 1 (ADM1), proposed by the International Water Association (IWA) (Batstone et al., 2002) in 2002, was created to establish a common platform for modelling the anaerobic digestion processes (Kleerebezem, 2006). The challenger today is to develop mathematical models to understand the dynamics of the processes, improve system performance and the optimize digesters in their design stage (Lauwers et al., 2013). Although studies have recently been published to address these objectives, in the case of APFRs, due to their relatively recent implementation, there is an important gap in the literature (Donoso-Bravo et al., 2018).

The primary aim of this work is the application of a mathematical model for anaerobic plug flow reactors based on the use of tank reactors with simple geometry, continuous flux and an absence of turbulence, and with diffusion and advection the only transport mechanisms along the flow. The second aim is to assess the effectiveness of the model based on the results. A third aim is to consider the potential of this methodology for the localization of each of the model variables within the system, for the undertaking of comparative studies of the different variables, and for modification of their behaviour in accordance with the geometry of the reactor and the different boundary values.

The proposed problem has a significant complexity. A description of it is made using the advection-diffusion-reaction equation (ADRE) and the boundary value problem (BVP). The ADRE is a nonlinear, second-order partial differential equations (PDE) based on mass balance. The difficulty to obtain theoretical solutions of these transport equations is due, firstly, to the nonlinear coefficients and terms of the ADRE and, secondly, to the complexity of a process in which several reactions take place simultaneously and whose variables depend on both the point within the reactor and the time considered.

The use of Galerkin's formulation of the finite element method (FEM) offers a great advantage compared to other methods because of its efficient modelling of vector fields by computational calculations (Aragonés et al., 2019). This allows an analysis of the relationships between a large number of variables involved in the process in a reasonably short time (Aragonés et al., 2019;Brito-Espino et al., 2019). The FEM is one of the most popular and powerful numerical techniques for solving transient parabolic-type PDEs (Lin and Reutskiy, 2018; Bozkurt et al., 2000). FEMs typically incorporate (approximate) continuity/conformity of the state variable(s) directly into the finite element space in order to reproduce the respective properties of the corresponding continuous problem (Georgoulis and Pryer, 2018).

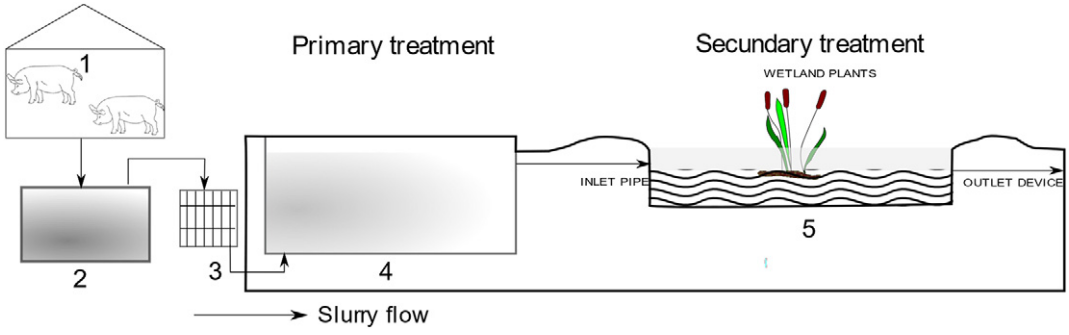

Fig. 1. Example of a systematic flow diagram of a farm wastewater treatment plant, based on both anaerobic digester and constructed wetlands systems, installed in different pig farms in Gran Canaria (Spain) (Mendieta-Pino et al., 2019). Pig house; (2) storage for raw swine slurry; (3) wire mesh; (4) anaerobic plug-flow reactor; (5) constructed wetland.

2. Mathematical model

2.1. Governing equations

As noted in the Introduction section, the joint use of anaerobic reactors and CWs (Fig. 1) improves the overall operating performance of these natural treatment systems. For these cases, a mathematical model is therefore proposed that includes the necessary physical, chemical and biological phenomena. It is intended as a useful tool in the design of theses such systems. The physical phenomenon corresponds to the transport of mass immersed in fluid by advection and diffusion, and the chemical and biological processes are essentially the kinetics of different metabolites. These phenomena may be defined or idealized by a set of relationships between multiple variables in the form of equations in partial derivatives. These variables are classified as dependent variables, such as fluid velocity ($\vec{v}$) or metabolites concentration (ϕ), and independent variables which are mainly connected with the geometry of the system and consequently, with the point of the physical space and with the time.

The mathematical model that describes the heterogeneous system is the ADRE. The ADRE problem consists of determining a function of scalar field, $\phi(x_i,t)$, which must satisfy the differential Eq. (1).

$$\frac{\partial \phi}{\partial t} \quad \mathfrak{D}\Delta\phi + \vec{u}\frac{\partial \phi}{\partial x_i} + f(\phi) = F(x_i)\ for\ x_i \epsilon \Omega \tag{1}$$

where (ϕ) is a scalar field that represent concentrations of both substrates and cells of each of the biochemical reactions included in the anaerobic processes, ($\vec{u}$) is the velocity field associated with the advective process and is obtained through the steady-state Stokes equations in two dimensional domains (4), x_i are Cartesian coordinates, t is the time of exposure, Ω is a polygonal or polyhedral domain in $\mathbb{R}^d$; for this study a two-dimensional problem is considered and so d = 2, $\mathfrak{D}$ is the diffusive coefficient; in this case the value considered $\mathfrak{D} = \mathfrak{D}_x = \mathfrak{D}_y =$ is a constant, Δ is the Laplace operator, a differential operator given by $\sum_{i=1}^{d}\frac{\partial^2}{\partial x_i^2}$, $f(\phi)$ is the external force applied to the system (>0 source, and <0 sink), $F(x_i)$ is a generation function.

Furthermore, ADRE must also satisfy the boundary values defined by Eqs. (2) and (3):

$$\phi(x_i,t) = g_D(x_i)\ for\ x_i \epsilon \Gamma_D \subset \partial\Omega, t>0 \tag{2}$$

$$\frac{\partial \phi(x_i,t)}{\partial n} n(x_i) = g_N(x_i)\ for\ x_i \epsilon \Gamma_N \subset \partial\Omega, t>0 \tag{3}$$

where $g_D(x_i)$ is the function which describes the scalar field value on the boundary, the Dirichlet boundary value problem, $g_N(x_i)$ is the function which describe the flow value on the boundary, the Neumann boundary value problem (Fig. 2-a), $\partial\Omega$ is the boundary of the domain, and n is the (typically exterior) normal to the boundary.

The Dirichlet boundary value problem was defined in the model by fully restraining the top, bottom and in some areas, both sides (Fig. 2-b).

2.1.1. Stokes equations

The Stokes equation in two dimensions (1) is used to calculate the velocity vector ($\vec{u}$). This is a linear PDE system used to determine the flow of viscous fluids for very low Reynolds numbers. Its relationship with the Navier-Stokes equations is based on the Stokes equation being a stationary linearization of this.

The governing equations, or strong form, of the steady-state Stokes equation are shown in (4) and (5):

to find $\vec{u} = (u_1, u_2)$ and p such that:

$$-\nu\Delta\vec{u} + \nabla p = \vec{f}\ for\ x,y \epsilon \Omega \tag{4}$$

$$\nabla\vec{u} = 0\ for\ x,y \epsilon \Omega \tag{5}$$

where $\vec{u} = (u_1, u_2)$ represents the velocity, p is the pressure, ν the viscosity coefficient, and $\vec{f}$ an external force that affects the system. Eq. (5) expresses the continuity equation for a stationary flux.

Furthermore, Stokes equations must also satisfy both the Neummann and Dirichlet boundary value problems defined by Eqs. (6) and (7):

$$\vec{u} = \vec{u}_0\ for\ x,y \epsilon \Gamma_D \tag{6}$$

$$\nabla\vec{u} \cdot n + pn = g\ for\ x,y \epsilon \Gamma_N \tag{7}$$

A general analytical solution is not available for this equation, so the FEM is used to find an approximation of the solution.

2.1.2. Anaerobic processes. Kinetic model

The ADM1 is used for the description of the function $f(\phi)$ (1). In this model, ϕ refers to the scalar field, such as concentration of substrate (S_i) and active anaerobic biomass (X_i). The ADM1 is based on sewage sludge anaerobic digestion and gives a unified representation of disintegration, hydrolysis, acidogenesis, acetogenesis and methanogenesis. The model, which has been categorized into two biochemical and physicochemical frameworks, contains a total of 21 dynamic state variables from substrates and cells. The biochemical and physicochemical processes are represented in the Fig. 3.

The proposed expressions to describe the consumption of substrate and microbial growth for each biochemical process and for each point in the domain are given by:

$$f(S_i) = -\rho_j\frac{Xi}{Yi}; f(X_i) = \rho_j X_i - K_d Xi \tag{8}$$

where, $f(S_i)$ ($kg\ m^{-3}d^{-1}$) is the change in substrate concentration, X_i is the biomass concentration ($kg\ CODm^{-3}$), Y_1 is the substrate yield coefficient, $f(X_i)$ ($kgCODm^{-3}d^{-1}$) is the change in cell concentration over

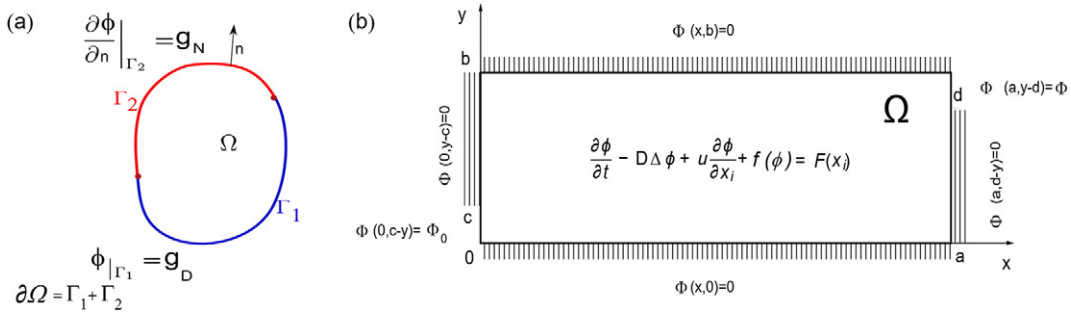

Fig. 2. (a) red: Neumann boundary value problem; blue: Dirichlet boundary value problem; boundary=$\partial\Omega = \Gamma_1 \cup \Gamma_2$; ϕ_0 and g are given function defined on Γ_1 *and* Γ_2; n = unit normal vector. (b) Dirichlet boundary value problem for the ADRE in the proposed model.

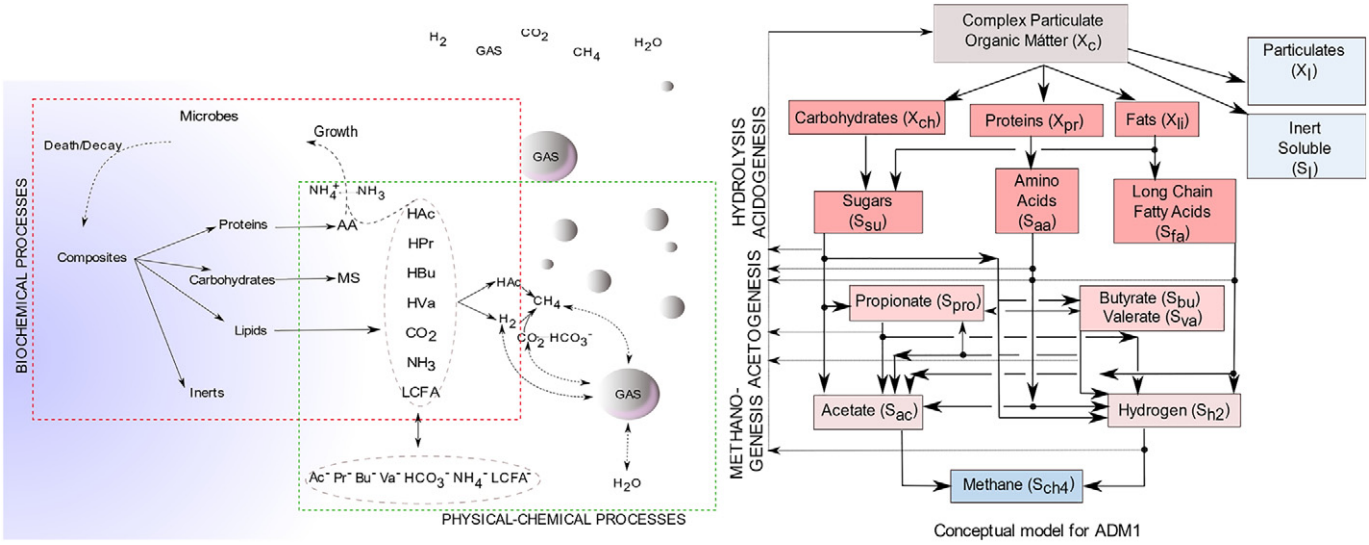

Fig. 3. Biochemical and physicochemical processes in anaerobic digestion (left), ADM1 conceptual model (right) (Batstone et al., 2002).

time, and $Kd(d^{-1})$ is the cell decay rate. The specific growth rate; ρ_j (d^{-1}), is based on the monod-type reaction kinetics (Batstone et al., 2002);

$$\rho_j = \mu_{max_i}\frac{S_i}{K_{S_1}+S_i}\cdot X_i \cdot I_1 \cdot I_2 \cdots I_n \tag{9}$$

where μ_{max_i} (d^{-1}) is the maximum specific growth rate, $S_i(kg\ m^{-3})$ the substrate concentration, K_{S_1} $(Kg\ m^{-3})$ is the substrate saturation constant (*i.e.* substrate concentration at half, and μ_{max}), I_i; is the different inhibition function considered (Table 2).

2.2. The finite element method for the proposed model

Considering the transient and steady-state problems given by (1), for a general $F(x_i)$ it may be difficult or even impossible to find ϕ with analytical techniques, and so it is necessary to use numerical techniques and, in particular, the finite elements method (FEM).

The FEM method is a numerical technique based on the generation of a finite element geometric model on which the methodology is defined. The methodology consist of dividing the domain into a collection of subdomains, considering the differential equation of the problem as a variational equation defined in each of the subdomains. Next, in a rigorous order, all the equations of the each of the elements are linked into a global system of equations -weak formulations- for the final calculation (2.2.1).

2.2.1. Variational formulation

The variational equation is obtained:

- by multiplying (1) by the test functions (Y_i) and (4) and (5) by the test functions $\overrightarrow{v}$ and g, respectively. The test functions and solutions ϕ are assumed to belong to Hilbert spaces. A Hilbert space is an infinite-dimensional function space with functions of specific properties that can be suitably managed in the same way as ordinary vectors in a vector space.
- the next step consists of integrating both sides of equality in (1), in (4) and in (5). With the techniques of integration by parts and the boundary value problem, it is reasonable to get linear partial derivative equations.

In obtaining this weak formulation, the existence of solutions for Eqs. (1), (4) and (5) is ensured. This is known as the weak solution of the initial equation or strong formulation.

- The weak forms of the ADRE problems of (4) change as follow:

to find $\phi \in H_0^1$ such that:

$$\begin{aligned}
&\int_\Omega \frac{\partial \phi}{\partial t}\cdot Y_i + \mathfrak{D}\int_\Omega \nabla\phi\cdot\nabla Y_i + \int_\Omega u\nabla\phi\cdot Y_i + \int_\Omega f(\phi)\cdot Y_i = F(x_i)\cdot Y_i \quad for\ \ all\ \ Y_i \in H_0^1(\Omega)\\
&\phi(x_i,t) = g_D(x_i) \qquad for\ \ x_i \in \Gamma_D \subset \partial\Omega, t>0\\
&\frac{\partial\phi(x_i,t)}{\partial n} n(x_i) = g_N(x_i) \qquad for\ \ x_i \in \Gamma_N \subset \partial\Omega, t>0
\end{aligned} \tag{10}$$

where Y_i is the smooth function and H_0^1 is the Hilbert space.

- The weak forms of the Stokes equation of (4) are:

to find $\overrightarrow{u} = (u_1, u_2)$ and $p \in [H_0^1(\Omega)]^2$ and $p \in L^2(\Omega)$ such that:

$$\begin{aligned}
&\mu\int_\Omega \nabla\overrightarrow{u}\cdot\nabla\overrightarrow{v} - \int_\Omega \left(div\ \ \overrightarrow{v}\right)p = \int_\Omega \overrightarrow{f}\,\overrightarrow{v} \quad for\ \ all\ \ \overrightarrow{v} \in \left[H_0^1(\Omega)\right]^2,\\
&\int_\Omega \left(div\ \ \overrightarrow{u}\right)q = 0 \qquad for\ \ all\ \ q \in L^2(\Omega),\\
&\overrightarrow{u}(x,y) = \overrightarrow{h}_D(x,y) \qquad for\ \ x,y \in \Gamma_D\\
&\nabla\overrightarrow{u}\cdot n = \overrightarrow{h}_N(x,y) \qquad for\ \ x,y \in \Gamma_N
\end{aligned} \tag{11}$$

where $\overrightarrow{v}$ and g are the smooth functions and H_0^1 is the Hilbert space.

2.2.2. Galerkin formulation and finite element approximation

To obtain Galerkin formulation it is necessary, first, to build a more or less regular triangulation τ^h quasi-uniform in the domain Ω. This triangulation is composed of the elements K_i and the vertices x_i (as shown in Fig. 4) in order to create an appropriate discrete space $\tau^h \subset \Omega$. The finite dimension spaces defined for the model are shown in (12);

$$\begin{aligned}
\mathbb{P}^1\left(\tau^h\right) &= \{v \in C(\Omega) : v|_K \text{ is a po lynomial of total degree equal to } 1 \text{ for } K \in \tau^h\}\\
&\quad \{v \in C(\Omega) : v|_K = a + bx + cy\},\\
\mathbb{P}_0^1\left(\tau^h\right) &= \{v \in \mathbb{P}^1\left(\tau^h\right) : v(x) = 0 \text{ for } x \in \partial\Omega\}\\
\mathbb{P}^2\left(\tau^h\right) &= \{v \in C(\Omega) : v|_K \text{ is a polynomial of total degree equal to } 2 \text{ for } K \in \tau^h\}\\
&\quad \{v \in C(\Omega) : v|_K = a + bx + cy + dxy + ex^2 + fy^2\}\\
\mathbb{P}_0^2\left(\tau^h\right) &= \left\{v \in \mathbb{P}^2\left(\tau^h\right) : v(x) = 0 \text{ for } x \in \partial\Omega\right\}
\end{aligned} \tag{12}$$

For ADRE, ϕ_i must be located in the function space $\mathbb{P}^2(\tau^h)$, and the weak functions used are, $Y_i \in \mathbb{P}_0^2(\tau^h)$. For Stokes equation, $\overrightarrow{u}$ must be

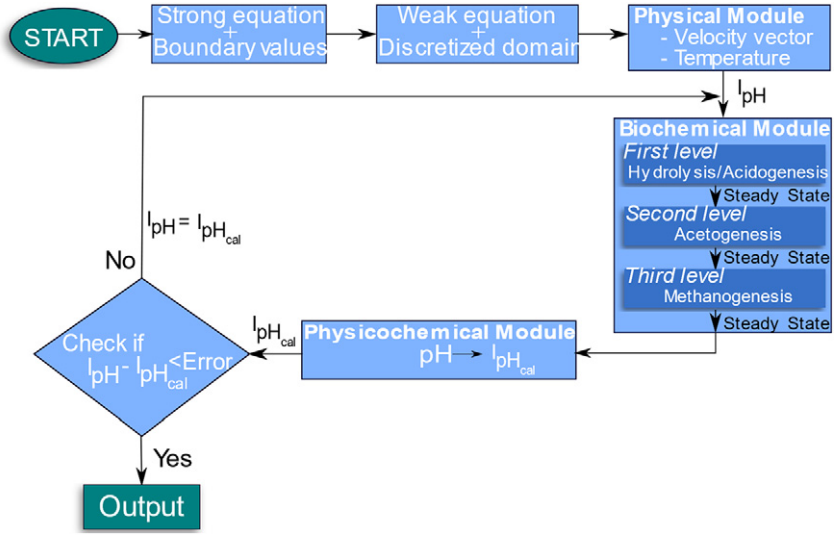

Fig. 4. Schematic representation of the anaerobic processes modelling framework.

located in the function space, $\mathbb{P}^2(\tau^h)$ and $p \in \mathbb{P}^1(\tau^h)$, and the weak functions used are, $v \in \mathbb{P}_0^2(\tau^h)$ and $q \in \mathbb{P}_0^1$, respectively (Zienkiewicz et al., 2000).

For all of this, and customizing ϕ_i= substrate (Si) and cells (Xi), the Galerkin formulation is as follows:

- ADRE
  - for substrate.

To find $S_i \in H_0^1(\Omega)$ *such that*:

$$\begin{aligned}
&\frac{1}{\Delta t}\int_\Omega Si_m \cdot Yi + \mathfrak{D}\int_\Omega \nabla Si_m \cdot \nabla Yi + \int_\Omega u\nabla SiYi = \\
&\int_\Omega \left(\rho_j Xi\right) Yi + \frac{1}{\Delta t}\int_\Omega Si_{m-1} Yi && \text{for all } Y_i \in \mathbb{P}_0^2\left(\tau^h\right) \\
&S_i(0,(x,y)) = S_{i_0}(x,y) && \text{for } x,y \in \Omega_1\ BC \\
&S_i(x,y,t) = g_D(x,y) && \text{for } x,y \in \Gamma_D \subset \partial\Omega, t>0 \\
&\nabla S_i(x,y,t) n(x,y) = g_N(x,y) && \text{for } x,y \in \Gamma_N \subset \partial\Omega, t>0
\end{aligned} \tag{13}$$

  - for cell.

To find $X_i \in H_0^1(\Omega)$ *such that*:

$$\begin{aligned}
&\frac{1}{\Delta t}\int_\Omega Xi_m \cdot Yi + \mathfrak{D}\int_\Omega \nabla Xi_m \cdot \nabla Yi + \int_\Omega u\nabla XiYi = \\
&\int_\Omega \left(\rho_j Xi - K_d Xi\right) Yi + \frac{1}{\Delta t}\int_\Omega Xi_{m-1} Yi && \text{for all } Y_i \in \mathbb{P}_0^2\left(\tau^h\right) \\
&X_i(0,(x,y)) = X_{i_0}(x,y) && \text{for } x,y \in \Omega_1 \\
&X_i(x,y,t) = g_D(x,y) && \text{for } x,y \in \Gamma_D \subset \partial\Omega, t>0 \\
&\nabla X_i(x,y,t) n(x,y) = g_N(x,y) && \text{for } x,y \in \Gamma_N \subset \partial\Omega, t>0
\end{aligned} \tag{14}$$

Δt is the discretization of time obtained from the Taylor series; $\frac{\partial Xi}{\partial t}(t,x) \simeq \frac{Xi(t+\Delta t,x) - Xi(t,x)}{\Delta t}$, $Xi_m = Xi(t+\Delta t,x)$, $Xi_{m-1} = Xi(t,x)$.

- Stokes equations:

to find $\vec{u} = (u_1, u_2) \in \mathbb{P}^2(\tau^h)$ and $p \in \mathbb{P}^1(\tau^h)$ such that:

$$\begin{aligned}
&\mu\int_\Omega \nabla\vec{u} \cdot \nabla\vec{v} - \int_\Omega \left(\ div\ \vec{v}\right) p = \int_\Omega \vec{f}\,\vec{v} && \text{for all } \vec{v} \in \mathbb{P}_0^2\left(\tau^h\right), \\
&\int_\Omega \left(\ div\ \vec{u}\right) q = 0 && \text{for all } q \in \mathbb{P}_0^1\left(\tau^h\right), \\
&\vec{u}(x,y) = \vec{h}_D(x,y) && \text{for } x,y \in \Gamma_D \\
&\nabla\vec{u} \cdot n = \vec{h}_N(x,y) && \text{for } x,y \in \Gamma_N
\end{aligned} \tag{15}$$

2.3. Modelling; framework

The general framework used for the description of the model is shown in Fig. 4.

1. Once the governing equations and boundary values are defined, the next step is the development of the weak formulation and the building of the mesh for the different domains considered (Fig. 5).
2. In the physical module, calculation is made of the velocities and the temperature field in steady state.
3. The biochemical module is divided into three levels and the methodology is as follows:
   (a) Substrate and cell concentrations are calculated at the first level until the steady state is reached: carbohydrate, proteins, fats, sugars, aminoacids and long-chain fatty acids.
   (b) The product of the above reactions becomes a source for the calculation of substrate concentrations at the second level: propionate, butyrate, valerate.
   (c) With the product of the reactions at the first and second levels the procedure continues in the same way as in the previous cases: acetate.
4. In the physicochemical module the pH values are calculated for each point in the system, I_{pH}, and then the resulting factor factors resulting ($I_{pH_{cal}}$). These values are compared with the initial I_{pH} and their convergence will give us the final result.

To select an optimal mesh it was decided to increase the number of nodes for the whole set of domains considered, since each of the processes is carried out in different parts of the system. For this reason, the total number of nodes chosen for the configuration of the mesh was 5399 (Fig. 5). This increase offers a more realistic simulation of the dispersion and the advection processes in the anaerobic reactor and, in addition, it can be assumed that pollutant removal and microbial kinetics is better represented.

2.4. Tools

There are many commercial software applications available for simulations. The vast majority have been developed for the simulation of specific cases. Among the most robust and widely accepted are CWM1, CW2D and BIO-PORE (Sams'o and Garcia, 2013) for constructed wetlands, and Matlab, BioWin and COMSOL Multiphysics for full-mix anaerobic fermentation systems. However, fewer models are available

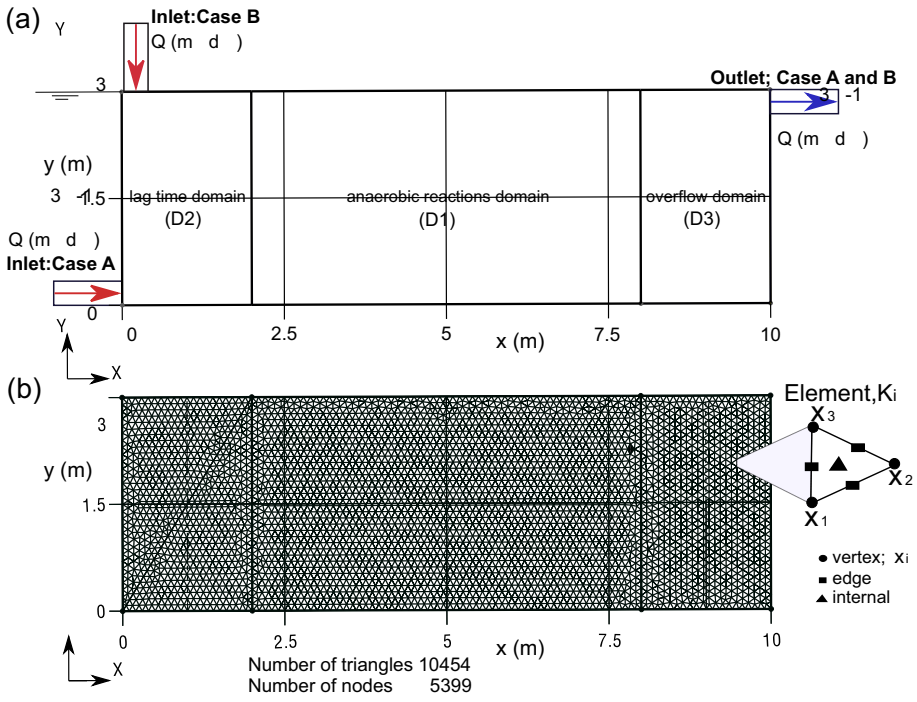

Fig. 5. (a) Geometric characteristics of the model under consideration and the different domains contemplated in it; (b) Polygonal discretization (H_0^1) showing an element (Ki) with the corresponding degrees of freedom.

for the simulation of free water surface wetlans and some of these include a limited number of components and interactions (Gargallo et al., 2017).

FreeFem++ was used to implement the algorithm for the calculation. It is a PDE solver which uses the FEM with its own high level language (Hecht, oi:10.15,15/jnum-2012-0013). FreeFem++ has object-oriented prograing language elements similar to C++. Freefem++ has many advantages; it is an open access software, has a powerful generated mesh, and it has a large collection package to visualize approximate solutions. Its scripts can solve multiphysics non linear systems in 2D and 3D (Herus et al., 2018).

3. Results and discussion

The numerical simulations of the model were performed considering two different cases, according to the location of the flux inlet pipe and the direction of the flow (Fig. 5). Case A: location - lower left side, flow - parallel to the x-axis. Case B, location - top left side, flow - parallel to the y-axis. The outlet pipe, for both Cases A and B, was located on the top right side and was parallel to the x-axis.

The start-up conditions and boundary values considered are as follows;

1. The system is subject to a continuous and constant flow with a value of $Q = 9m^3 \cdot d^{-1}$.
2. The operating time of the system is $T = 60$ days, a period in which the steady state of all the biochemical processes attained.
3. The diffusion coefficient is $\mathfrak{D} = 8.64 \cdot 10^{-3} m^2 \cdot d^{-1}$.
4. The system consists of three domains (Fig. 5): D1 - anaerobic reaction domain, D2 - lag time domain (there is no microbial activity due to its adaptation to the environment), D3 - overflow domain (in which it is considered that there are no anaerobic reactions).
5. The kinetic and physicochemical parameters used are reported in Table 1, and the biological inhibition factors in Table 2.
6. The boundary value in the inlet for substrate concentrations is $Si = 100g(COD) \cdot l^{-1}$ and for cells $Xi = 0.05g(COD) \cdot l^{-1}$ (Table 3).
7. Source values: propionate, butyrate, valerate, long-chain fatty acids and acetate are the products of biochemical reactions whose values are obtained from the stoichiometric relationship in which they form part (Table 3).

More detailed information about these expressions are given in the supplementary material and the parameter values can be found in the work of Batstone et al., 2002 and Zhang et al., 2015.

3.1. Hydraulic flow simulation

The flow simulation for Cases A and B after application of the steady-state Stokes equations (subsection 2.1.1) can be seen in Fig. 3. The maximum value of the velocity vector at the inlet and outlet points is $3m \cdot d^{-1}$, and in the rest of the domain an average velocity of $0.4m \cdot d^{-1}$ is maintained.

As can be seen, the trajectory drawn by the velocity vector is longer in Case A than in Case B.

Given that, for this model, the proposed geometric section is rectangular, regular meshing is proposed throughout the defined domains (see Fig. 5). As is clear in the simulations (Fig. 6), there is a regular distribution of the velocity vectors. If the geometry were to be changed, the methodology would remain the same, as the model is independent of the adopted geometry. In this case, the meshing can be refined with, for example, the nodes closer together in those areas where more definition is required (narrowing, singular points, etc).

It is important to reiterate that the advection-diffusion-reaction equation of the model describes the relationship between hydraulic, physical, biochemical and physicochemical properties. Using this methodology, by modifying the geometry it is possible to design flow so that the different processes take place in a certain location within the reactor, thereby improving biochemical reactions.

3.2. Distribution of the biomass and substrates

In this section, the behaviour of the biomass and substrates inside the system is evaluated. They are represented in steady state in Fig. 7

Table 1
Kinetic and physicochemical parameters.

Kinetic parameters	Sugar	Fats	Amino acids	Propionate	Butyrate	LCFA	Valerate	Acetate
$\mu_{max} d^{-1}$	6.9	3.9	6.9	0.49	0.67	6.1	1.1	7.5
$K_d d^{-1}$	0.9	1	1	0.04	0.03	0.25	0.04	0.037
$K_s kg(COD)/m^3$	0.5	0.8	3	1.145	0.176	0.8	0.5	0.037
Physicochemical parameters								
$K_a kmol/m^3$	CO_2	NH_3	Kw	propionate	butyrate	LCFA		
or $kgCOD/m^3$	6.35	9.25	14	4.88	4.82	4.86		

Table 2
Inhibition expressions used and constants according to the experimental data (Batstone et al., 2002). K_I=inhibition parameter; S = process substrate; S_I=inhibitor concentration; X = process biomass.

Description	Equation	Inhibition constant
free ammonia inhibition	$I_{IN} = \frac{S_I}{S_I + K_I}$	$K_I = 0.01$
total ammonia limitation	$I_{NH_3} = \frac{1}{1 + \frac{S}{K_1}}$	$K_I = 0.001$
pH inhibition	$I = \frac{1 + 2 \times 10^{0.5(pH_{LL} - Ph_{UL})}}{1 + 10^{pH - pH_{UL}} + 10^{pH_{LL} - pH}}$	$pH_{LL} = 6$; $pH_{UL} = 8.5$
Butyrate and valerate competition for C_4	$I = \frac{1}{1 + \frac{S_I}{S}}$	

for the simultaneously occurring acidogenesis (a), acetogenesis (b) and methanogenesis (c), considering Case A. It can be seen how cell growth and total consumption of the substrate takes place within the anaerobic reaction domain (Fig. 5(a)).

The simulations show different locations in the substrate bulk for the acidogenesis of sugars, the acetogenesis of butyrate and the methanogenesis of acetate. Similarly, the bacteria groups operate in separate spaces. Sugar concentrations, with a value of $Si = 100g(COD) \cdot l^{-1}$ at the inlet pipe, are completely removed, between the values of x = 2 and x = 3, while butyrate and acetate appear as products of the previous biochemical reactions (Fig. 3). The maximum values attained for butyrate and acetate are $Si_{but} = 12g(COD) \cdot l^{-1}$ and $Si_{acet} = 100g(COD) \cdot l^{-1}$, respectively. Both are removed in the mid-zone of the reactor.

The maximum biomass concentrations, due to the abundance of substrate, are located: in the acidogenesis between the value of x = 2 and x = 3, with a maximum value of $Xi = 0.21g(COD) \cdot l^{-1}$; in the acetogenesis between the value of x = 4.5 and x = 8.4, with a maximum value of $Xi = 0.7g(COD) \cdot l^{-1}$; and in the methanogenesis, between the value of x = 4.8 and x = 8.4, with a maximum value of $Xi = 7.4\ g(COD) \cdot l^{-1}$. The inlet value for all of them is $Xi = 0.5g(COD) \cdot l^{-1}$ and the residual value are: $Xi_{acidogenesis} = 0$, $Xi_{acetogenesis} = 0.1$, $Xi_{methanogenesis} = 7.4\ g(COD) \cdot l^{-1}$.

The higher concentration of bacteria benefits from the substrate intensification, the product of the biochemical reaction in the previous phases, acidogenesis/acetogenesis. Once the substrate has been removed, the bulk of the cells start to reduce due to their decay advection and diffusion (Fig. 7).

The results show the potential of the model, namely its ability to perform calculations for multiple processes, some occurring at the same time and others at different times, and whose results depend on each other. Evidence for this can be seen in Fig. 7 which allows identification of the different areas of the system where the biochemical and physicochemical reactions take place, and whose distributions are influenced by the diffusion and advection processes. The shape of cell distribution (Fig. 7, *Xi*) indicates a reasonable relationship with the rest of the colonies and with its substrates. The methodology allows a representation to be made of the distribution of the colonies with some coherence. This enables actions to be carried out in areas of the digester where they are needed to achieve certain improvements including, for example, temperature control at specific points to regulate the growth of particular previously selected cells. In general, the model is able to predict, for all the points of the system, the concentrations of each of the biochemical variables, the pH and the biogas production.

3.3. Comparison of two specific cases

By comparing the results obtained in substrate simulations for Cases A and B, described above, and considering the acidogenesis, acetogenesis, and methanogenesis (Fig. 8 (a) and (b)), a higher efficiency can be observed for substrate removal in Case A. In Case B, especially in acetogenesis and methanogenesis, part of the substrate, butyrate and acetate, reaches the outlet without being removed. Their values are $Si_{but} = 0.5g(COD) \cdot l^{-1}$ and $Si_{acet} = 2g(COD) \cdot l^{-1}$.

A graphical representation of both Cases is shown in Fig. 8-(c) through the AA axis. It is located at a height of 1.5 m and parallel to the x-axis (Fig. 8 (c)). As can be seen, in acidogenesis, no significant difference is found between the two cases. However, in the other phases there is approximately a 17% of increase in the concentrations of substrate. The relative displacement between both curves, Case B *vs.* Case A, shows the bulk of the substrate dragged to the right of the domain, with maximum concentration values of $Si_{but} = 12g(COD) \cdot l^{-1}$ and $Si_{acet} = 100g(COD) \cdot l^{-1}$, respectively.

As is clear from Fig. 8, it can be deduced that the inlet pipe location in an anaerobic plug flow reactor has a significant impact on substrate removal efficiency. Changes in the boundary values have an important

Table 3
Boundary value problems and sources for anaerobic processes: $Si = 100g(COD) \cdot l^{-1}$, $Xi = 0.05g(COD) \cdot l^{-1}$.

CASE	Sugar	Fats	Proteins	Propionate	Butyrate	LCFA	Valerate	Acetate
Inlet Substrate	S_i	S_i	S_i	–	–	–	–	–
Inlet Cells	X_i	X_i	X_i	X_i	X_i	X_i	X_i	X_i
Source	–	–	–	S_{ipro}	S_{ibu}	S_{ifa}	S_{iva}	S_{iac}

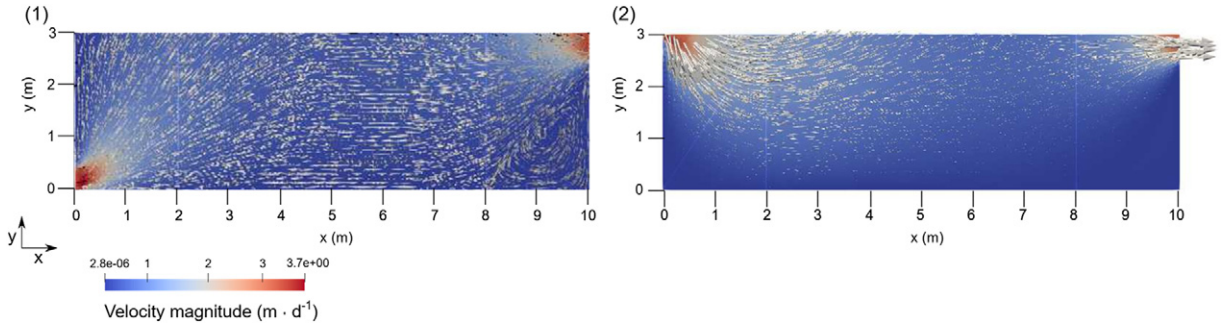

Fig. 6. Flow simulation results; (1) Case A and (2) Case B.

effect on the efficiency of microbial reactions in the removal of organic matter. One of the advantages of the model is that it can be used to compare different solutions to a problem, depending on the boundary values to which they are subject. The simulations allow a comparison of various situations and, in this way, enable improvements to the operating conditions of the reactor.

Freefem++ is an excellent tool for solving this kind of problem due to its calculating speed and accuracy, facilitating comparative studies of different options in a rapid and precise manner.

3.4. Effectiveness in the conservation of microorganisms

The simulations, along the axis AA, of the microorganisms involved in the different phases of the anaerobic processes are shown in Fig. 9. This axis is at a height of 1.5 m and in the direction of the x-axis (Fig. 9 -(h)).

The values of the concentrations at the inlet pipe, of each of the microorganisms that take part in the anaerobic digestion process, are equal to $Xi = 0.05g(COD) \cdot l^{-1}$. The highest concentration values achieved in steady state in $g(COD) \cdot l^{-1}$ are: $Xi_{sugar} = 7.5, Xi_{protein} = 24, Xi_{triglyceride} = 0.19, Xi_{butyrate} = 0.65, Xi_{propionate} = 0.65, Xi_{valerate} = 0.23, Xi_{acetate} = 0.5$. As shown in Fig. 9, the bulk concentrations in acidogenesis are located in the range of x = 1–3 ((a), (b), (c)), in acetogenesis x = 5–8 ((d), (e), (f)) and in methanogenesis x = 6.5–8 ((g)).

In order to preserve the survival of bacteria communities in the system, a feedback point could be established to return a portion of the fluid to the inlet pipe. Based on the results obtained from the graphs, the feeding points, selected for this case, are located at the distance of 2–3 m for the acidogenesis, 5–5.5 m for the acetogenesis and 6.5–8 m for the methanogenesis along the AA axis.

It should be pointed out that, in the present paper, the concentration profiles of the different variables are compared along the AA axis. The possibility of obtaining charts along different axes is available through this methodology. For this reason, with this approach, a systematic study of the stability of the cell colonies and its different survival areas can be made.

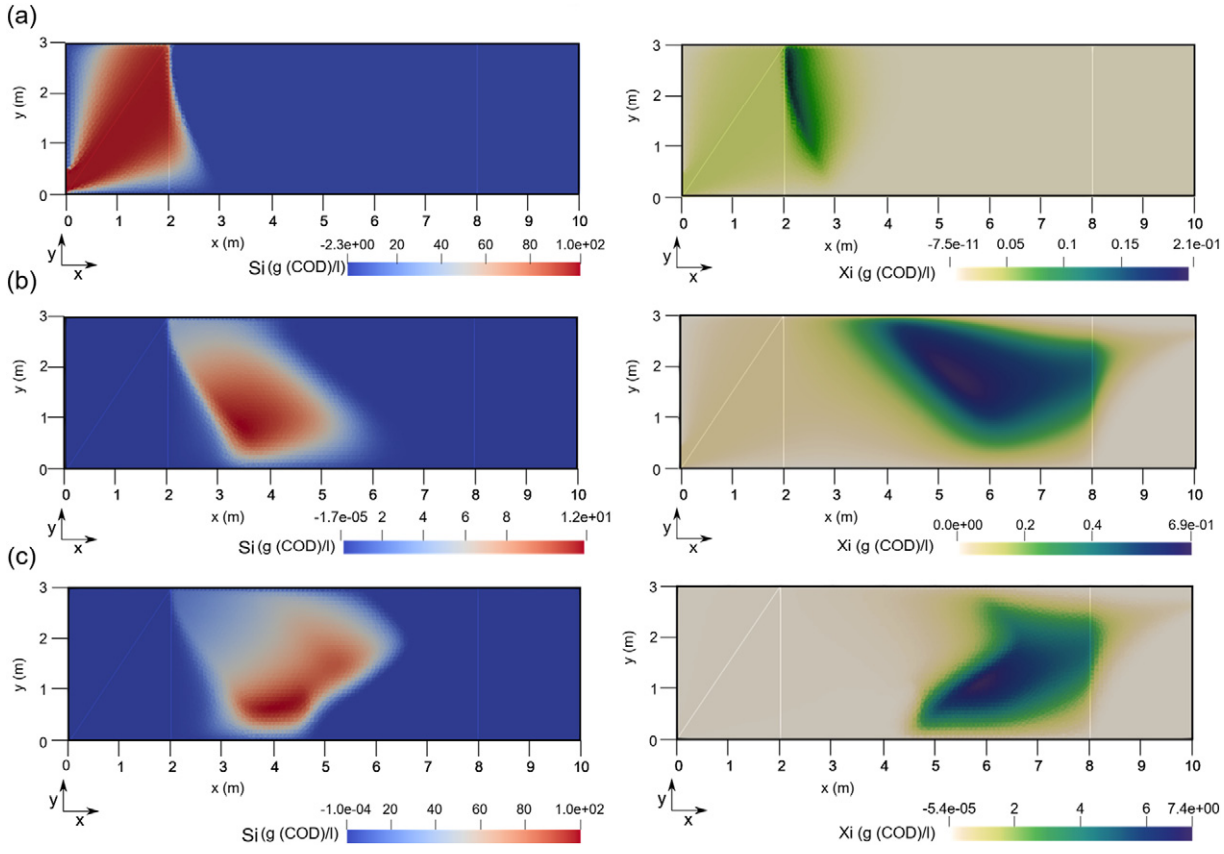

Fig. 7. Simulated substrates (Si) and cells (Xi) for (a) acidogenesis of sugar, (b) acetogenesis of butyrate, (c) methanogenesis of acetate.

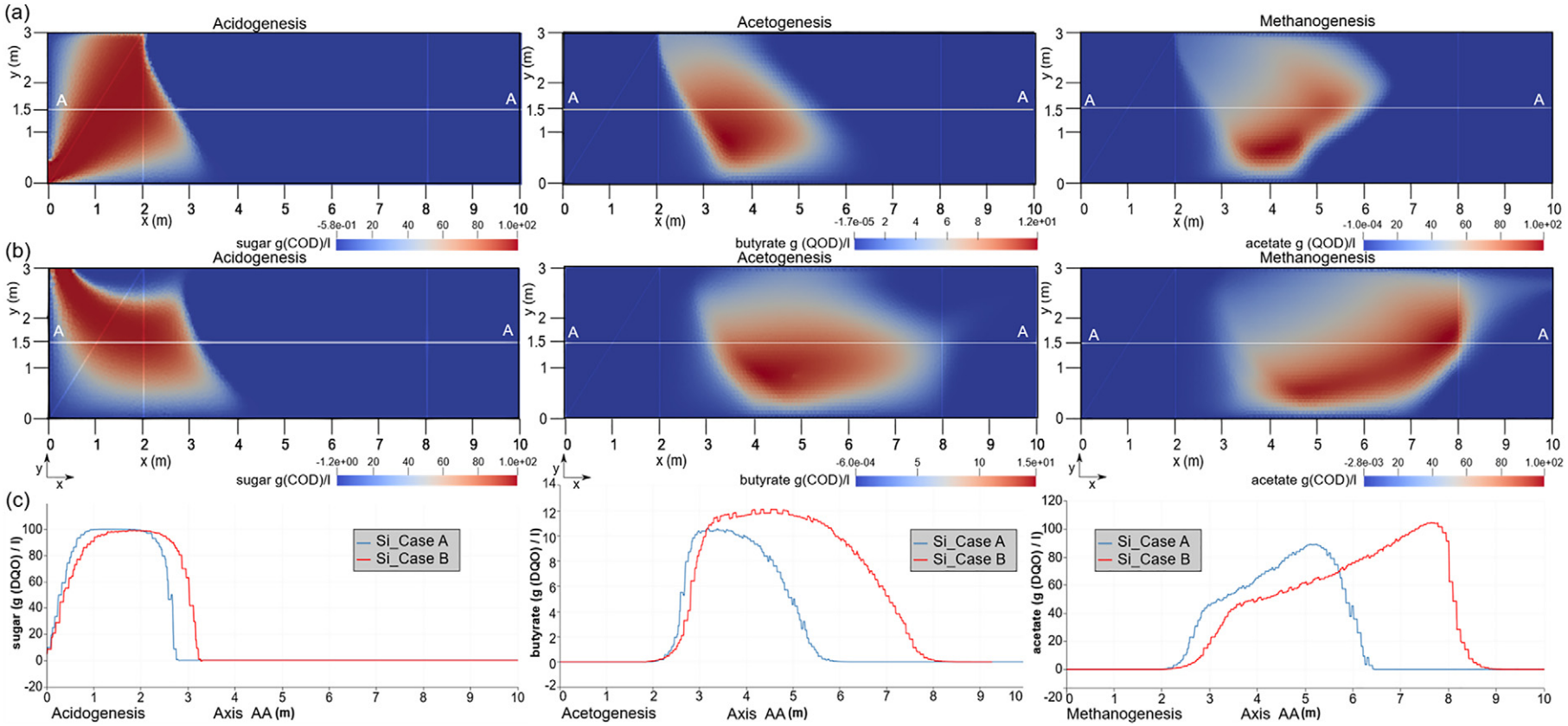

Fig. 8. Simulations of substrate in acidogenesis, acetogenesis and methanogenesis for two cases, according to the location of the inlet pipe; (a) Case A: on the lower left side (b) Case B: on the top left side.

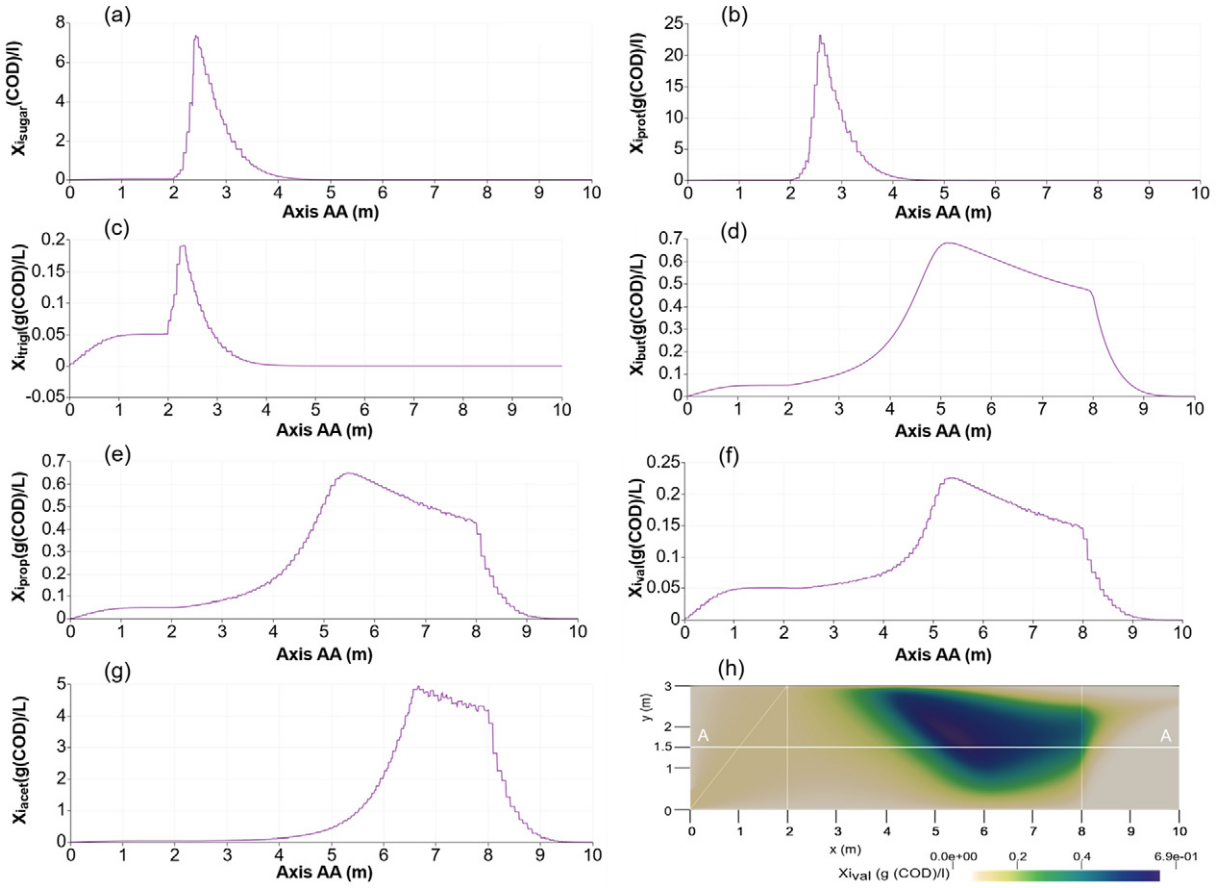

Fig. 9. Longitudinal profiles of the biomass along the AA axis (reflected in (h)) for the different processes. Acidogenesis for sugars (a), proteins (b) and fats (c); acetogenesis for butyrate (d), propionate (e) and valerate (f); and methanogenesis FOR acetate (g).

4. Conclusions

A mathematical model for wastewater treatment in anaerobic-plug flow reactors was developed in this work to describe the complex behaviour of a high number of simultaneous reactions in a heterogeneous fluid within a digester subject to continuous and constant flow. This model satisfactorily links biochemical and physicochemical reactions to the physical and hydraulic properties through Stokes equations and the advection-diffusion-reaction equations where ADM1 has been implemented. In total,21 variables were considered. The resulting partial differential equations of the model, both linear and nonlinear, were treated by the Galerkin finite element formulation. The results were facilitated by the development of a flowchart and the use of the open access software Freefem++, an effective tool for applying the finite element method due to its calculating speed and accuracy. In the light of the results, the potential of this methodology for calculating multiple biochemical and physicochemical reactions is evidenced. By visualizing datasets through their simulations, it can show the different areas where these reactions take place within the system. With this methodology it is also possible to design flows according to the geometry of the reactor so that the chemical and physicochemical reactions can be carried out in certain suitable areas within the digester. The possibility, with this methodology, of representing the distribution of the anaerobic cells with some coherence enables actions to be carried out in some areas of the digester to improve their performance. In general, the model is able to predict, for all the points of the system, the concentrations of each of the biochemical variables, the pH and the biogas production. Another advantage of the model is that it can be used to compare different solutions of a problem, depending on the boundary values to which they are subject. Finally, the fundamentals of the model are generally valid with a certain accuracy, even if the reality of the problem is not reflected. Future applications of the model include the possibility of optimizing the anaerobic digestion process through the incorporation in the model of the effects of radiation, temperature and wind.

Declaration of competing interest

The authors declare that they have no known competing financial interests or personal relationships that could have appeared to influence the work reported in this paper.

Acknowledgements

This research has been co-funded by the INTERREG V-A Cooperation, Spain-Portugal MAC (Madeira-Azores-Canarias) 2014-2020 programme, MITIMAC proyect (MAC2/1.1a/263)

Appendix A. Supplementary data

Supplementary data to this article can be found online at https://doi.org/10.1016/j.scitotenv.2019.136244.

References

Alvarez, J., Ru´ız, I., Soto, M., 2008. Anaerobic digesters as a pretreatment for constructed wetlands. Ecological Engineering 33, 54–67 URL. http://www.sciencedirect.com/science/article/pii/S0925857408000293 https://doi.org/10.1016/j.ecoleng.2008.02.001.

Aragonés, L., Pagán, J., López, I., Navarro-González, F., Villacampa, Y., 2019. Galerkin's formulation of the finite elements method to obtain the depth of closure. Science of The Total Environment 660, 1256–1263 URL. http://www.sciencedirect.com/

science/article/pii/S004896971930018X https://doi.org/10.1016/j.scitotenv.2019.01.017.

Batstone, D., Keller, J., Angelidaki, I., Kalyuzhnyi, S., Pavlostathis, S., Rozzi, A., Sanders, W., Siegrist, H., Vavilin, V., 2002. The iwa anaerobic digestion model no 1 (adm1). Water Sci. Technol. 45, 65–73. URL: http://wst.iwaponline.com/content/45/10/65, arXiv:http://wst.iwaponline.com/content/45/10/65.full.pdf.

Bozkurt, S., Moreno, L., Neretnieks, I., 2000. Long-term processes in waste deposits. Science of The Total Environment 250, 101–121. http://www.sciencedirect.com/science/article/pii/S0048969700003703 https://doi.org/10.1016/S0048-9697(00)00370-3.

Brito-Espino, S., Mendieta-Pino, C., Pérez-Báez, S., Ramos-Martín, A., 2019. Application of a model-based method for hydrodynamic processes in constructed wetland to management of livestock wastewater based on finite elements method. Desalin. Water Treat. 152, 92–98. https://doi.org/10.5004/dwt.2019.23940.

Comino, Elena, Riggio, Vincenzo A., M.R., 2013. Constructed wetland treatment of agricultural effluent from an anaerobic digester. Ecological Engineering 54, 165–172 URL. http://www.sciencedirect.com/science/article/pii/S0925857413000426 https://doi.org/10.1016/j.ecoleng.2013.01.027.

Donoso-Bravo, A., Sadino-Riquelme, C., Gómez, D., Segura, C., Valdebenito, E., Hansen, F., 2018. Modelling of an anaerobic plug-flow reactor. process analysis and evaluation approaches with non-ideal mixing considerations. Bioresource Technology 260, 95–104. http://www.sciencedirect.com/science/article/pii/S0960852418304449 https://doi.org/10.1016/j.biortech.2018.03.082.

Gargallo, S., Martín, M., Oliver, N., Hernández-Crespo, C., 2017. Biokinetic model for nitrogen removal in free water surface constructed wetlands. Science of The Total Environment 587-588, 145–156. http://www.sciencedirect.com/science/article/pii/S0048969717303376 https://doi.org/10.1016/j.scitotenv.2017.02.089.

Georgoulis, E.H., Pryer, T., 2018. Recovered finite element methods. Computer Methods in Applied Mechanics and Engineering 332, 303–324. http://www.sciencedirect.com/science/article/pii/S0045782517307764 https://doi.org/10.1016/j.cma.2017.12.026.

Hartl, M., Bedoya-Ríos, D.F., Fernández-Gatell, M., Rousseau, D.P., Laing, G.D., Garf ı, M., Puigagut, J., 2019. Contaminants removal and bacterial activity enhancement along the flow path of constructed wetland microbial fuel cells. Science of The Total Environment 652, 1195–1208 URL. http://www.sciencedirect.com/science/article/pii/S0048969718341305 https://doi.org/10.1016/j.scitotenv.2018.10.234.

Hecht, F., oi:10.15,15/jnum-2012-0013. n.d. New development in freefem++. J. Numer. Math., 20(3–4), pp. 251–266, (Retrieved 24 Sep. 2018, from d) .

Herus, V.A., Ivanchuk, Martyniuk, N., P.M., 2018. A system approach to mathematical and computer modeling of geomigration processes using freefem++ and parallelization of computations. Cybern. Syst. Anal. 54, 284–292 URL. https://doi.org/10.1007/s10559-018-0030-3.

Hu, C., Yan, B., Jun Wang, K., Min Xiao, X., 2018. Modeling the performance of anaerobic digestion reactor by the anaerobic digestion system model (adsm). J. Environ. Chem. Eng. 6, 2095–2104 URL. http://www.sciencedirect.com/science/article/pii/S2213343718301398 https://doi.org/10.1016/j.jece.2018.03.018.

Imfeld, G., Braeckevelt, M., Kuschk, P., Richnow, H.H., 2009. Monitoring and assessing processes of organic chemicals removal in constructed wetlands. Chemosphere 74, 349–362. http://www.sciencedirect.com/science/article/pii/S0045653508012095 https://doi.org/10.1016/j.chemosphere.2008.09.062.

Ivanovs, K., Spalvins, K., Blumberga, D., 2018. Approach for modelling anaerobic digestion processes of fish waste. Energy Procedia 147, 390–396. http://www.sciencedirect.com/science/article/pii/S1876610218302650 https://doi.org/10.1016/j.egypro.2018.07.108 international Scientific Conference “Environmental and Climate Technologies”, CONECT 2018, 16-18 May 2018, Riga, Latvia.

Kleerebezem, 2006. Critical analysis of some concepts proposed in adm1. Water Sci. Technol. 54 (4), 51–57.

Kumar, J., Zhao, Y., 2011. A review on numerous modeling approaches for effective, economical and ecological treatment wetlands. Journal of Environmental Management 92, 400–406. http://www.sciencedirect.com/science/article/pii/S0301479710004159 https://doi.org/10.1016/j.jenvman.2010.11.012.

Kythreotou, N., Florides, G., Tassou, S.A., 2014. A review of simple to scientific models for anaerobic digestion. Renew. Energy 71, 701 – 714. URL: http://www.sciencedirect.com/science/article/pii/S0960148114003164, doi:https://doi.org/10.1016/j.renene.2014.05.055.

Laitinen, J., Moliis, K., Surakka, M., 2017. Resource efficient wastewater treatment in a developing area—climate change impacts and economic feasibility. Ecological Engineering 103, 217–225. http://www.sciencedirect.com/science/article/pii/S0925857417301817 https://doi.org/10.1016/j.ecoleng.2017.04.017.

Lauwers, J., Appels, L., Thompson, I.P., Degre've, J., Impe, J.F.V., Dewil, R., 2013. Mathematical modelling of anaerobic digestion of biomass and waste: power and limitations. Prog. Energy Combust. Sci. 39, 383 – 402. URL: http://www.sciencedirect.com/science/article/pii/S0360128513000178, doi:https://doi.org/10.1016/j.pecs.2013.03.003.

Lin, J., Reutskiy, S., 2018. An accurate meshless formulation for the simulation of linear and fully nonlinear advection diffusion reaction problems. Advances in Engineering Software, 127–146. http://www.sciencedirect.com/science/article/pii/S0965997817308268 https://doi.org/10.1016/j.advengsoft.2018.08.012.

Mendieta-Pino, C.A., Ramos-Martin, A., Perez-Baez, S.O., Brito-Espino, S., 2019. Management of slurry in gran canaria island with full-scale natural treatment systems for wastewater (ntsw). one year experience in livestock farms. Journal of Environmental Management 232, 666–678. http://www.sciencedirect.com/science/article/pii/S0301479718313380 https://doi.org/10.1016/j.jenvman.2018.11.073.

Regmi, P., Stewart, H., Youri Amerlinck, E.A., 2019. The future of WRRF modelling- outlook and challenges. Water Sci. Technol. 79 (1), 3–14.

Rossi, D., Gargiulo, L., Valitov, G., Gavriilidis, A., Mazzei, L., 2017. Experimental characterization of axial dispersion in coiled flow inverters. Chemical Engineering Research and Design 120, 159–170. http://www.sciencedirect.com/science/article/pii/S0263876217300977 https://doi.org/10.1016/j.cherd.2017.02.011.

Sams'o, R., Garcia, J., 2013. Bio-pore, a Mathematical Model to Simulate Biofilm Growth and Water Quality Improvement in Porous Media: Application and Calibration for Constructed Wetlands. 54 pp. 116–127.

Sanchez-Ramos, D., Agullo´, N., Sams´o, R., Garc´ıa, J., 2017. Effect of key design parameters on bacteria community and effluent pollutant concentrations in constructed wetlands using mathematical models. Science of The Total Environment 584-585, 374–380 URL. http://www.sciencedirect.com/science/article/pii/S0048969717300141 https://doi.org/10.1016/j.scitotenv.2017.01.014.

Union, E., 2008. Green paper on the management of bio-waste in the European Union. URL. https://eur-lex.europa.eu/legal-content/EN/TXT.

de la Varga, D., Ruiz, I., Alvarez, J., Soto, M., 2015. Methane and carbon dioxide emissions from constructed wetlands receiving anaerobically pretreated sewage. Science of The Total Environment 538, 824–833 URL. http://www.sciencedirect.com/science/article/pii/S0048969715305933 https://doi.org/10.1016/j.scitotenv.2015.08.090.

Wang, M., Zhang, D.Q., Dong, J.W., Tan, S.K., 2017. Constructed wetlands for wastewater treatment in cold climate. a review. Journal of Environmental Sciences 57, 293 311 URL. http://www.sciencedirect.com/science/article/pii/S1001074217303108 https://doi.org/10.1016/j.jes.2016.12.019.

Wu, H., Zhang, J., Ngo, H.H., Guo, W., Hu, Z., Liang, S., Fan, J., Liu, H., 2015. A review on the sustainability of constructed wetlands for wastewater treatment: Design and operation. Bioresource Technology 175, 594–601. http://www.sciencedirect.com/science/article/pii/S0960852414014904 https://doi.org/10.1016/j.biortech.2014.10.068.

Zhang, Y., Piccard, S., Zhou, W., 2015. Improved adm1 model for anaerobic digestion process considering physico-chemical reactions. Bioresource Technology 196, 279 289 URL. http://www.sciencedirect.com/science/article/pii/S0960852415010275 https://doi.org/10.1016/j.biortech.2015.07.065.

Zienkiewicz, O., Taylor, R., Taylor, R., Taylor, R., 2000. The Finite Element Method: The basis. Fluid Dynamics. Butterworth-Heinemann URL. https://books.google.es/books?.

water

Article

A Framework Based on Finite Element Method (FEM) for Modelling and Assessing the Affection of the Local Thermal Weather Factors on the Performance of Anaerobic Lagoons for the Natural Treatment of Swine Wastewater

Saulo Brito-Espino *,†, Alejandro Ramos-Martín †, Sebastian O. Pérez-Báez †, Carlos Mendieta-Pino † and Federico Leon-Zerpa †

Department of Process Engineering, Institute for Environmental Studies and Natural Resources (i-UNAT), University of Las Palmas de Gran Canaria (ULPGC), 35017 Las Palmas, Spain; alejandro.ramos@ulpgc.es (A.R.-M.); sebastianovidio.perez@ulpgc.es (S.O.P.-B.); carlos.mendieta@ulpgc.es (C.M.-P.); federico.leon@ulpgc.es (F.L.-Z.)

* Correspondence: saulo.brito101@alu.ulpgc.es

† These authors contributed equally to this work.

Abstract: Anaerobic lagoons are natural wastewater treatment systems suitable for swine farms in small communities due to its low operational and building costs, as well as for the environmental sustainability that these technologies enable. The local weather is one of the factors which greatly influences the efficiency of the organic matter degradation within anaerobic lagoons, since microbial growth is closely related to temperature. In this manuscript, we propose a mathematical model which involves the two-dimensional Stokes, advection–diffusion-reaction and heat transfer equations for an unstirred fluid flow. Furthermore, the Anaerobic Digestion Model No1 (ADM1), developed by the International Water Association (IWA), has been implemented in the model. The partial differential equations resulting from the model, which involve a large number of state variables that change according to the position and the time, are solved through the use of the Finite Element Method. The results of the simulations indicated that the methodology is capable of predicting reasonably well the steady-state of the concentrations for all processes that take place in the anaerobic digestion and for each one of the variables considered; cells, organic matter, nutrients, etc. In view of the results, it can be concluded that the model has significant potential for the design and the study of anaerobic cells' behaviour within free flow systems.

Keywords: modelling; anaerobic digestion; ADM1; free flow reactors; finite elements analysis

check for updates

Citation: Brito-Espino, S.; Ramos-Martín, A.; Pérez-Báez, S.O.; Mendieta-Pino, C.; Leon-Zerpa, F. A Framework Based on Finite Element Method (FEM) for Modelling and Assessing the Affection of the Local Thermal Weather Factors on the Performance of Anaerobic Lagoons for the Natural Treatment of Swine Wastewater. *Water* **2021**, *13*, 882. https://doi.org/10.3390/w13070882

Academic Editor: Bing-Jie Ni

Received: 1 February 2021
Accepted: 11 March 2021
Published: 24 March 2021

1. Introduction

Anaerobic digestion (AD) is an eco-friendly biological process which is universally used for the treatment of agricultural, industrial and municipal wastewater around the world [1–4]. Its utilization is increasingly widely, due to its capacity for producing methane, which can be used afterwards as a heat source or for electricity generation, taking part within the low-carbon energy technologies and circular bio-economy [5]. In this context, anaerobic lagoons (AL) are natural wastewater treatment systems with a long hydraulic retention time, suitable for small communities due to the low energy demand and the operating costs [6–9]. By applying this kind of technology, the mechanical equipment, used for mixing processes in conventional plants, are avoidable. In addition, AL offer a number of advantages, such as the establishment of concentration profiles along the reactor, a buffering capacity in cases of overloads and greater protection against acidification [10]. However, due to the fact that AD is strongly influenced by temperature, there is a close dependence between AL and weather conditions, so its implementation may be limited in cold or low solar radiation areas [8,11].

The application of mathematical models builds understanding for both microbial-related dynamic and kinetic processes, reveals optimisation possibilities, which lastly improves the digester's performance [12,13]. The IWA Anaerobic Digestion Model No.1 (ADM1) [14], created in 2002 to stablish a common platform for the modelling of AD processes [15], has been widely applied in waste treatment processes, due to its high feasibility, considering the fact that most of the processes of AD are included within ADM1 [16]. However this model has merely been applied to completely mixed reactors. The approach of models based on the ADM1 for unstirred waste water treatment systems has been little studied. In these models, complexity is increased and the effect of boundary conditions is essential. Moreover, the mathematical complexity required by these models does not entail a significant issue, due to the increasing technological and computational development [12].

In the past twenty years many researches based on mathematical models for treatment processes in lagoons have been carried out. Fleming [17] created the first models applying computational fluid dynamic (CFD) for the prediction of the performance of full-scale incompletely mixed anaerobic digesters. Wu and Chen [8] developed a CFD model for AL which combines physical and biological processes, and includes both heat conduction and solar radiation by a thermal model. In this model, a single-phase incompressible Newtonian fluid is considered. Goodarzi, Sookhak Lari, and Mossaiby [18] determined the effect of ambient and inlet temperature variations on the hydraulic performance of a typical rectangular pond. In all these described models, the biological processes are depicted by a single equation depending on the concentrations of the influent and effluent. Brito-Espino, Ramos-Martín, Pérez-Báez, and Mendieta-Pino [19] defined advection, diffusion and reaction phenomena for wastewater treatment in anaerobic plug flow reactors by non-linear, second order, partial differential equations. ADM1 is implemented within this model, and both biochemical and physical–chemical reactions of ADM1 are calculated by a flowchart for sequential processes. In this method, temperature is not considered. Nevertheless, very few researches have been conducted to develop a comprehensive model which integrates fluid flow, heat transfer, and cells behaviour in AL.

The aim of this work is to set-up a theoretical framework for wastewater treatment in unstirred flow anaerobic lagoons, by a model which allows the integration of fluid flow, heat transfer and cells behaviour, for the purpose of describing processes occurring in AL. The implementation of the ADM1 into the model and the consideration of the influence of the local thermal weather, identified with the boundary conditions, allows the model to portray the processes taking place in reality more precisely than [19]. In order to do this, an improved two dimensional mathematical model, based on the coupling of a set of parabolic partial differential equations (PDEs) and related to the phenomena associated to AL, has been developed. In addition, Dirichlet, Neumann and Robin boundary conditions have been established on the differential equations. This model combines the parametrization of different processes within the lagoon and its environment with the finite element analysis. Finally, the parallelization of the resulting algorithm has been performed in the simulation, therefore allowing an improved computational efficiency than the resulting form sequential processes in [19]. Thanks to the help of FreeFemm++ and the parallel solver package, available for this software, the processing of each one of the variables related to AD processes and the simultaneous exchange of the data has been feasible. Having said this, we conclude that the novelty of this study resides in the following aspects. Firstly, in the implementation of the ADM1 and the heat transfer phenomenon in a mathematical model which describes a unstirred fluid flow, in order to predict the spatial distribution of the different variables that take part in the processes within the AL. Furthermore, secondly, in the optimisation and designing of the algorithm, by parallel method, providing an accurate forecast of the real behaviour of the process, as is shown in the ADM1. In the simulation, two different scenarios have been chosen as examples; the first corresponds to a conventional AL which is subjected to the ambient temperature, and the second includes

heat sources, induced by solar assisted [20] or through the biofuel recovery in the anaerobic process [21,22].

2. Materials and Methods

2.1. Overview

Pollutant is removed in AL through combination of physical, biochemical and physical–chemical phenomena. Advection, diffusion and heat transfer are the most common physical processes in these systems (Figure 1). Both the organic matter and the suspended microorganism within lagoons are subjected to the mechanical transport with the bulk flow of the water (advection). At the same time, they tend to spread out and diffuse from higher to lower concentration as time varies (diffusion). The energy transfer in the system, due to a temperature gradient (heat transfer), is performed by conduction and convection processes. Atmospheric factors associated with the borders of the model on the Earth's surface include, beside the two previous, radiation process. Digestion process is carried by anaerobic microorganism's activity, bacteria an archaea, through a number of sequential and parallel reactions. The biochemical reactions consist of irreversible five-stage processes; disintegration, hydrolysis, acidogenesis, acetogenesis and methanogenesis reactions. Physical–chemical reactions are those reversible processes where cells are not involved. They are, firstly, the ion association/dissociation, and gas–liquid transfer [14].

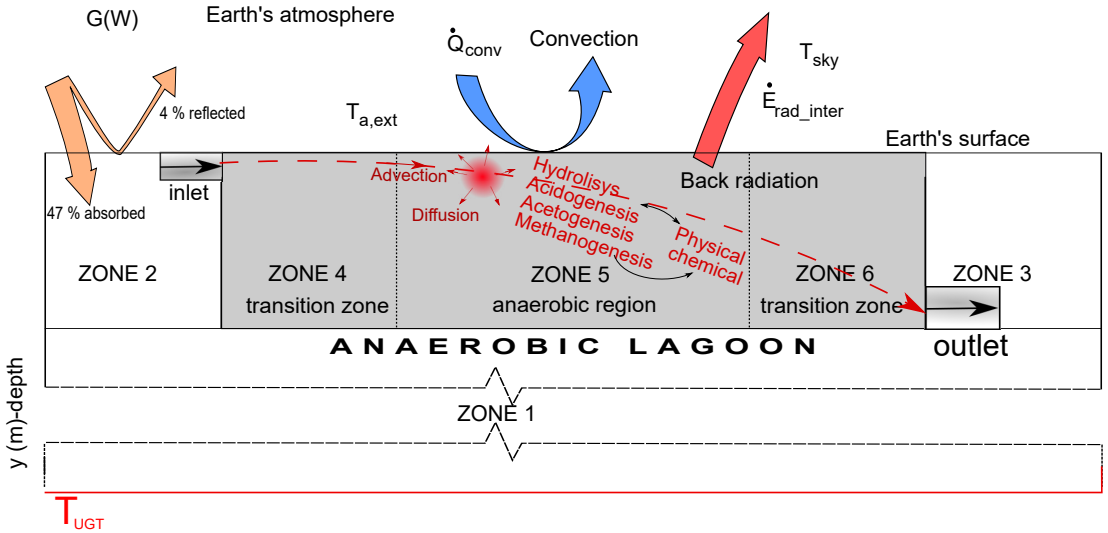

Figure 1. Scheme of the different phenomena that take places in AL and their environments.

Considering a system where the lagoon and its environment are included, different zones can be identified (Figure 1). Depending on the local parameters—thermal conductivity, specific heat, density, and where biological processes take place—they are considered different zones. Boundary conditions are located on the borders. Undisturbed ground temperature T_{UGT} is a ground thermal property situated at a depth where the ground temperature is approximately invariable, depth value depends on climatic conditions and is different in various regions of the Earth [23,24].

2.2. Governing Equations (Strong Formulations)

In this research, the mathematical model proposed is based on the two-dimensional advection–diffusion-reaction, Stokes, and heat transfer equations. This is accompanied by a series of boundary conditions. On the other hand, the IWA Anaerobic Digestion Model 1 (ADM1) has been implemented in the model.

The description of the model has been expressed in terms of primitive variables, mass, velocity, pressure, and temperature. In these equations it has been assumed that velocity and temperature field are in steady state conditions.

2.2.1. Advection–Diffusion Reaction Equation

Advection–diffusion-reaction Equation (ADRE) as numerical solution, widely used within mathematical modelling, to describe physical, biochemical and physical–chemical processes in AL [19,25–27].

Governing equations and boundary conditions are summarized below.

$$\begin{aligned} \frac{\partial \phi}{\partial t} - \mathfrak{D}\Delta\phi + \vec{u}\,\nabla\phi + f(\phi) = F(x,y) \;\; for \;\; x,y \;\epsilon\; \Omega \\ \phi(x,y,t) = g_D(x,y) \;\; for \;\; x,y \;\epsilon\; \Gamma_D \subset \partial\Omega, t > 0 \\ \frac{\partial \phi(x,y,t)}{\partial n} n(x,y) = g_N(x,y) \;\; for \;\; x,y \;\epsilon\; \Gamma_N \subset \partial\Omega, t > 0 \end{aligned} \tag{1}$$

where (ϕ) is a scalar field that represent concentrations of both substrates and cells of each of the biochemical reactions included in the anaerobic processes, $\vec{u} = (u_1, u_2)$ is given by Equations (2), $f(\phi)$ is the source function, which is positive $f(\phi) > 0$ for growth and production or negative $f(\phi) < 0$ for decay and consumption, biomass and metabolites, respectively, Γ_D and Γ_N are Dirichlet and Neumann boundary conditions, respectively. This term is developed in Equation (7) , $F(x,y)$ is a generation function, which is zero (0) in this case.

2.2.2. Stokes Equation

Stokes equation, together with the ADR has been used to describe the flow. It is usually used for fluid with slowly motion and with high viscosity [28,29]. In this research, a constant density and incompressible Newtonian fluid flow has been considered. Strong formulation and Dirichlet Γ_D and Γ_N boundary conditions are as follow.

$$\begin{aligned} -\nu\Delta\vec{u} + \nabla p = \vec{F} \;\; for \;\; x,y \;\epsilon\; \Omega \\ \nabla\vec{u} = 0 \;\; for \;\; x,y \;\epsilon\; \Omega \\ \vec{u} = \vec{u_0} \;\; for \;\; x,y \;\epsilon\; \Gamma_D \\ \nabla\vec{u}\cdot n + pn = g \;\; for \;\; x,y \;\epsilon\; \Gamma_N \end{aligned} \tag{2}$$

2.2.3. The Energy Equation—Temperature Distribution

The energy equation is based on the conservation of energy and the Fourier heat conduction laws [30]. The internal energy balance equations, under a steady-state Eulerian description can be expressed as a function of temperature [30,31]

$$\begin{aligned} \rho_0 C_v(\vec{u}\,\nabla T) - \nabla(k_i \nabla T) = 0 \;\; for \;\; x,y \;\epsilon\; \Omega \\ T(x,y) = T_{aa}(x,y) \;\; for \;\; x,y \;\epsilon\; \Gamma_D \\ \frac{\partial T(x_i,t)}{\partial n} n(x_i) = g_N(x_i) \;\; for \;\; x,y \;\epsilon\; \Gamma_N \\ k\frac{\partial T}{\partial n} = h(T_{a,ext} - T) + \varepsilon_s \cdot \sigma \cdot (T^4 - T_{sky}^4) \;\; for \;\; x,y \;\epsilon\; \Gamma_R \end{aligned} \tag{3}$$

where Γ_D corresponds to Dirichlet condition. It is applied to the UGT (Figure 1); Γ_N is the Neumann condition. It describes the value of the gradient of the dependent field variable, normal to the boundary. Its calculation is based on Fourier Law; Γ_R is the Robin condition. It describes the Earth's surface heating and cooling Γ_R. This implied the use of Stefan–Boltzmann's law and Newtons' law of cooling to model the heat exchange, related to radiation and convection processes, respectively [32,33]. Stefan–Boltzmann constant is $\sigma = 5.68 \cdot 10^{-8} (\mathrm{W \cdot K^{-4} \cdot m^{-2}})$ [34]; $T_{a,ext}$temperature of the externally surrounding surface; ε_s is the Earths' surface emissivity, where $0 \leq \varepsilon_s \leq 1$; T_{sky} is the sky radioactive temperature. These are used to estimate the radiative heat exchange with the Earth's

atmosphere [35]. T_{sky} and ε_{sky} is used to estimate the radiative heat exchange with the Earth's atmosphere [35].

$$T_{sky} = \left(\frac{\varepsilon_{sky} \cdot T_{a,ext}^4}{\sigma} \right)^{\frac{1}{4}} - 273.15 \quad (4)$$

$$\varepsilon_{sky} = \left(0.787 + 0.764 ln \left(\frac{T_{dp}}{273} \right) \right) (1 + 0.0224N + 0.0035N^2 + 2.8 \cdot 10^{-4} N^3) \quad (5)$$

such $0 \leq \varepsilon_{sky} \leq 1$.

Here N are tenths cloud cover, and $T_{dp}(K)$ is the dew-point temperature to which it must be cooled to become saturated. It is obtained by a correlation found in [33] (6) and

$$T_{dp} = T - \left(\frac{100 - RH}{5} \right) \quad (6)$$

In this work, heat sources from biochemical reactions have not been considered.

2.2.4. Kinetic Equations

ADM1 is used for the description $f(\phi)$ (Equation (1)). Biochemical rate coefficients and kinetic rate equations are represented in the Tables S1 and S2 within the Supplementary Materials Section. First order kinetic was considered for the hydrolysis, acidogenesis, acetogenesis and methanogenesis. The following equations based on common kinetic expressions describe anaerobic treatment processes:

$$f(S_i) = -\frac{\partial S_i}{\partial t} = -\rho_j \frac{Xi}{Yi} \;\; ; \;\; f(X_i) = \frac{\partial X_i}{\partial t} = \rho_j X_i - K_d Xi \;\; ; \;\; \rho_j = \mu_{max_i} \frac{S_i}{K_{s_1} + S_i} \cdot I_1 \cdot I_2 \cdots I_n \quad (7)$$

$f(S_i)$ and $f(X_i)$ are the changes in substrates and cells concentration over time. These equations are based on the monod-type reaction kinetics [13,36]. In this model, it has been considered free ammonia and pH inhibitions, in addition to the butyrate and valerate competition [19].

The influence of temperature has been obtained by the Cardinal Temperature Model 1 (Appendix A) proposed by [37]

$$\mu_{max} = \mu_{opt} \frac{(T - T_{max})(T - T_{min})^2}{(T_{opt} - T_{min})[(T_{opt} - T_{min})(T - T_{opt}) - (T_{opt} - T_{max})(T_{opt} + T_{min} - 2T)]} \quad (8)$$

2.3. Solution Procedure

The finite element method, numerical technique based on the generation of a finite element geometric model, is used for the solution of the partial differential equations including in the problem.

In this methodology, the major steps include

1. The approach of the weak forms from the governing equations. The solutions are assumed to belong to Hilbert space, considering this space as an infinite dimensional function space with functions of specific properties that can be suitably managed in the same way as ordinary vectors in a vector space. They are represented in Table 1.
2. Discretization of the domains, both physical with more or less regular triangulation and related to time. In Figure 2, the discretization of the different sub-domains, nodes and triangle, is showed.
3. Selection of the shape functions, essential to provide an approximation of the solution within an element. These relate the coordinates of every point of a finite element with the positions of its nodes,
4. Formulation of the system of equations.
5. Solving systems of equations. The free software FreeFem++ has been used to solve them. It is a PDE solver with its own high-level programming language and accurate

syntax for mathematical formulation. Freefem++ have high diversity of triangular finite elements (linear and quadratic, Lagrangian elements, discontinuous P^2, etc.) to solve PDE in two (2D) and three (3D) dimensions.

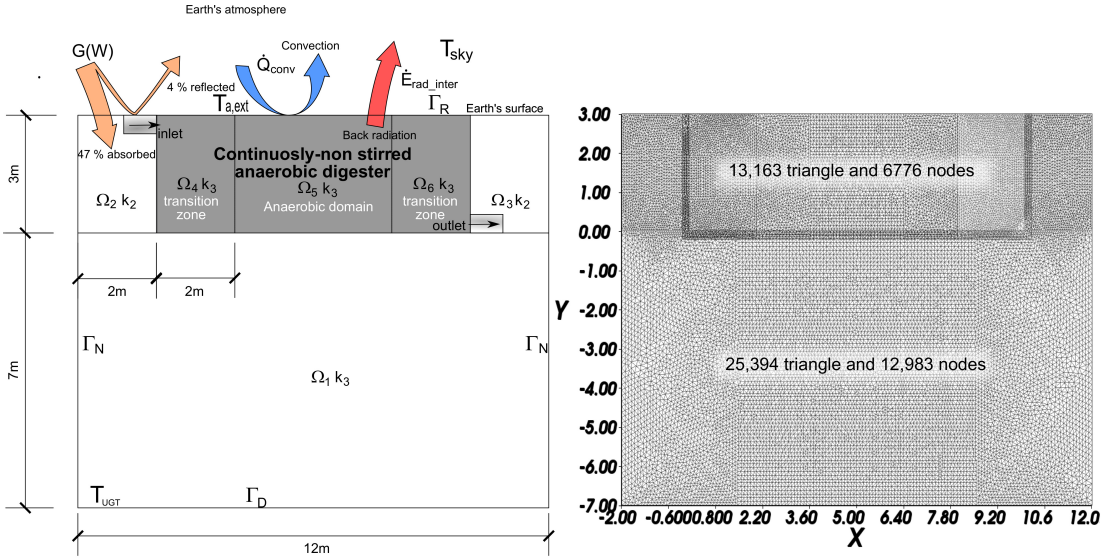

Figure 2. (**left**) geometric characteristics and boundary values; (**right**) dicretization of the domains.

Table 1. Scheme of the weak equations used in the model, where $\vec{v}, q, Y_i, W$ are the smooth functions and $\mathbb{H}_0^1, \mathbb{P}_0^1, \mathbb{P}_0^2$ are the Hilbert space.

Model	Weak Equations	Hilbert Spaces
Stokes	$\mu \int_\Omega \nabla \vec{u} \cdot \nabla \vec{v} - \int_\Omega (div\ \vec{v}) p = \int_\Omega \vec{f} \vec{v}$ $\int_\Omega (div\ \vec{u}) q = 0$	$for\ \ all\ \ \vec{v}\ \epsilon\ \mathbb{P}_0^2(\tau^h)$ $for\ \ all\ \ q\ \epsilon\ \mathbb{P}_0^1(\tau^h)$
ADR	$\int_\Omega \frac{\partial \phi}{\partial t} \cdot Y_i + \mathfrak{D} \int_\Omega \nabla \phi \cdot \nabla Y_i + \int_\Omega u \nabla \phi \cdot Y_i + \int_\Omega f(\phi) \cdot Y_i = F(x_i) \cdot Y_i$	$for\ \ all\ \ Y_i\ \epsilon\ \mathbb{H}_0^1(\Omega)$
Thermal	$\int_\Omega W \left[-\frac{\partial}{\partial x,y}(k \frac{\partial T}{\partial x,y} - \frac{\partial}{\partial xj}(k \frac{\partial T}{\partial xj}) - q_c(x,y,xj) \right] dxi$	$for\ \ all\ \ T\ \epsilon\ \mathbb{P}_0^2(\tau^h)$

2.4. Calculation

The partial differential equation solver FreeFem++ was used to implement the algorithm for the calculation. Due to it advantages, open access software with a powerful generated mesh and a large collection package to visualize approximate solutions, makes Freefem++ an ideal tool to solve complex partial differential equations [38]. Parallel calculation by parallel computing on clusters of personal computer has been achievable with a Message Passing Interface (MPI) within Freefem++.

3. Results and Discussion

3.1. Model's Considerations

In order to solve the formulated problem, fitted for a specific case, it has been necessary to stablish geometric conditions, physical properties, initial conditions and boundary values. A summary of these characteristics is represented in Figure 2, Tables 2–4 and in the Supplementary Materials Section.

The system has been divided in different domains and subdomains. Ω_1, Ω_2 and Ω_3 are included within Ω_g and refer to the immediate ground around of lagoon; whereas Ω_4, Ω_5 and Ω_6 in Ω_r and concern the lagoon. AD occurs in Ω_5 considering Ω_4 and Ω_6 as transition zones (Figure 2).

In this case, the proposed anaerobic lagoon is located in temperate zones and is subjected to the environmental thermal conditions considering that there are no thermal loads on the sides of the domains, so the ground heat flow is transmitted vertically.

Table 2. General parameters considered. Q represents hydraulic flow in the inlet and outlet pipe. S_i and X_i represent substrate and cell concentrations in the inlet pipe.

Thermal Constants						Diffusion Coefficient	Boundary Values		
$cos\Theta$ $(W \cdot m^{-2})$	h_{int} $(W \cdot m^{-2} \cdot K^{-1})$	σ $(W \cdot m^{-2} \cdot K^{-4})$	k_1	k_2 $(m^2 \cdot d^{-1})$	k_3	$\mathfrak{D}$ $m^2 \cdot d^{-1}$	Q $(m^3 \cdot d^{-1})$	S_i (mg (COD) $\cdot L^{-1}$)	X_i
0.29	10	$5.67 \cdot 10^{-8}$	2.3	3	0.02	$8.64 \cdot 10^{-3}$	0.5	28,000	110–150

Table 3. Kinetic parameters [6].

Kinetic Parameters	Sugar	Fats	Amino Acids	Propionate	Butyrate	LFCA	Valerate	Acetic Acid
$\mu_{opt}(d^{-1})$	6.9	3.9	6.9	0.49	0.67	6.1	1.1	7.5
$K_d(d^{-1})$	0.9	1	1	0.04	0.03	0.25	0.04	0.037
K_s(kg (COD)/m^3)	0.5	0.8	3	1.145	0.176	0.8	0.5	0.037

3.2. Evaluation on Performance of Temperature

Figure 3 shows the temperature distribution in the proposed system under steady-state conditions for some examples of wastewater treatment plants whose information is included in Table 4. The lagoon contour has been illustrated in the first graphic. It is of interest to observe how the thermal behaviour within the lagoon depends on the boundary conditions, but also the hydraulic flow that is subject to the boundary values in the inlet and outlet pipe.

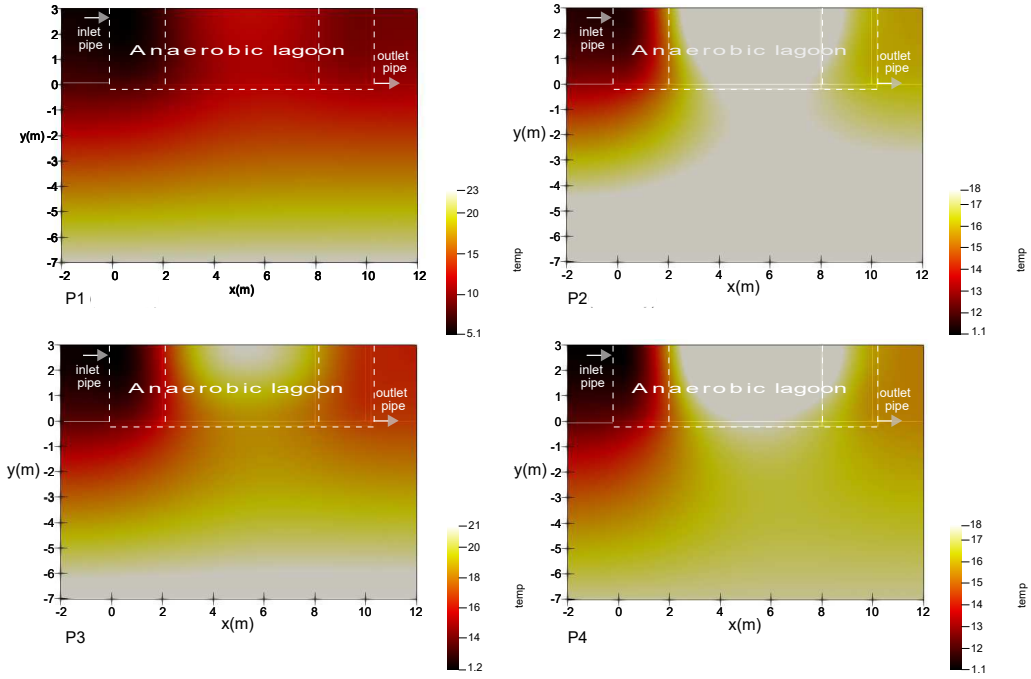

Figure 3. Temperature distribution under four different scenarios, according to the characteristic parameter exposed in Table 4.

Table 4. Specific weather parameters considered from four wastewater treatment plants (WWTP). It is provided the Universal Transverse Mercator (UTM) coordinates. T_{am} are the annual means temperatures and T_{mm} the monthly means. P1 and P3 are located in the coastal zones, while P2 and P4 are located in the mid-altitude zones.

WWTP	UTM Coordinate			wind ($m \cdot s^{-1}$)	T_{am} °C	T_{mm}	RH (%)	G (W/m^2)	T_{dp} (°C)	ε	T_{sky} (°C)
	x	y	z								
P1	430,371	3,108,919	11.60	6.6	22.7	19.0	64	290.53	11.8	0.822	5.00
P2	444,484	3,108,895	511	6.6	19.8	16.6	82	278.80	13.0	0.824	2.95
P3	428,778	3,084,390	271.81	5.3	22.2	19.3	66	299.39	12.5	0.823	5.41
P4	447,661	3,098,525	831.51	5.3	17.3	12.9	80	292.68	8.9	0.813	−1.53

3.3. Organic Matter Removal and Behaviour of the Microbial Community

Figure 4 represents the variation on concentrations, in steady state, happening in some of the processes taking place within the lagoon. These simulations describe, in the case of P1 (Table 4), the variation of sugar, propionate, acetic acid and their corresponding bacterial biomass concentration, along of the pond's length and depth, according to the boundary conditions as shown in Table 2.

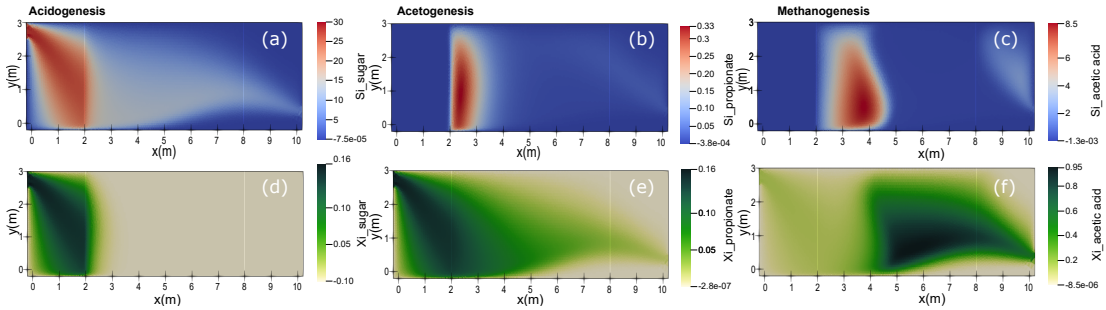

Figure 4. Concentrations' variation, together with the length and depth of the lagoon, for the example P1. (**a**–**c**) correspond to substrates, (**d**–**f**) to microorganisms.

As shown in these simulations, concentrations decreased throughout the pond length as a result of dispersion and biodegradation. The transition zones (Figure 2) have been considered as low microbial activity, so the net growth of cells is observable from the x-axis value equal to 2. As a result, propionate and acetic acid's source are located in this zone (Ω_5). The cells' growth is affected much more by the concentration of the substrates than the temperature's effects because temperature variations in this region differ very little from one point to another.

With respect to acidogenesis and methanogenesis, cells effectiveness on substrates removal is greater than in the acetogenesis due to the kinetic parameters. For the propionate μ_{max} and K_s are 0.49 (d^{-1}) and 1.145 $(mg(COD) \cdot m^{-3})$, respectively, (see Table 3). Thus, cells growth value and, therefore, the substrate removal is lower than in the previous two cases (see Equation (7)). The resulting value of substrate concentration in the outlet, after the wastewater treatment process, is between 600 and 500 (mg(COD)/L). In the case of acetic acid, this same concentration, next to the pond outlet, is smaller, due to the accumulation of organic matter that has not been reached by the microbial community.

Figure 5 shows charts representing substrate and propionic acid bacteria's concentrations for P1 (Table 4) along the axis AA. Cases 1 and 2, with different concentrations of microorganisms in the inlet pipe of the lagoon, 110 $(mg(COD) \cdot L^{-1})$ and 115 $(mg(COD) \cdot L^{-1})$, respectively, are compared. In both cases, the graphics share a similar trend, a downward slope which, al last, connects at the middle point of the axis. There is no net growth within the microbial population. The slope above mentioned is reduced, cells growth offsets the diffusion process in Ω_5 (Figure 2). Nevertheless, substrate removal in Case 2 is benefited by the highest concentration of cells at the inlet pipe 150 $(mg(COD) \cdot L^{-1})$. The decrease in values from the last section, for both graphs, occurs as a result of the dispersion phenomenon since microbial activity in Ω_6 has not been considered.

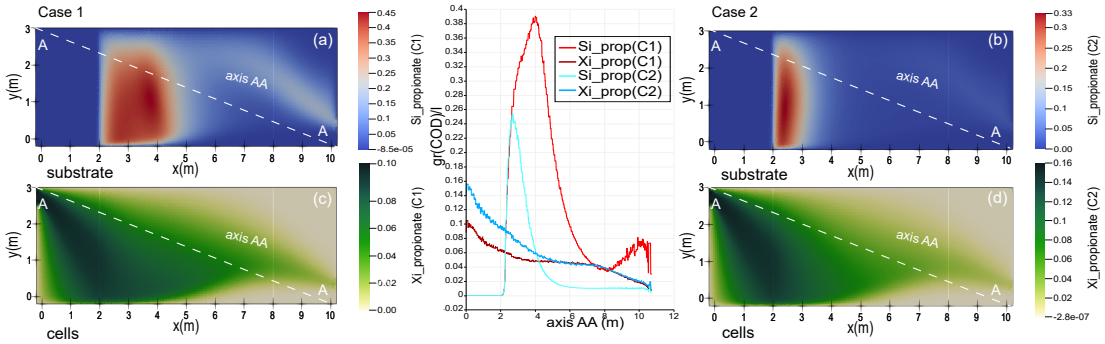

Figure 5. Performance of propionate, in steady state, for two different cases according to the initial concentration of propionic acetogenic bacteria and their graphic presentations along the axis AA. Case1; 110 (mg(COD) · L^{-1}), Case2; 115 (mg(COD) · L^{-1}).

Figure 6 depicts, as in the previous example, the chart of propionate along the axis AA as well as the distribution of temperature in the lagoon for three different examples. E-1; The lagoon is subjected to ambient temperature (see case P4 in Table 4 and Figure 3). E-2; It is included a bed heat source at the bottom of the lagoon, between 2 and 3 coordinates of the x axis with a temperature of 35 °C. E-3; In this occasion, that same heat source is located between coordinates 4 and 8 of the x axis.

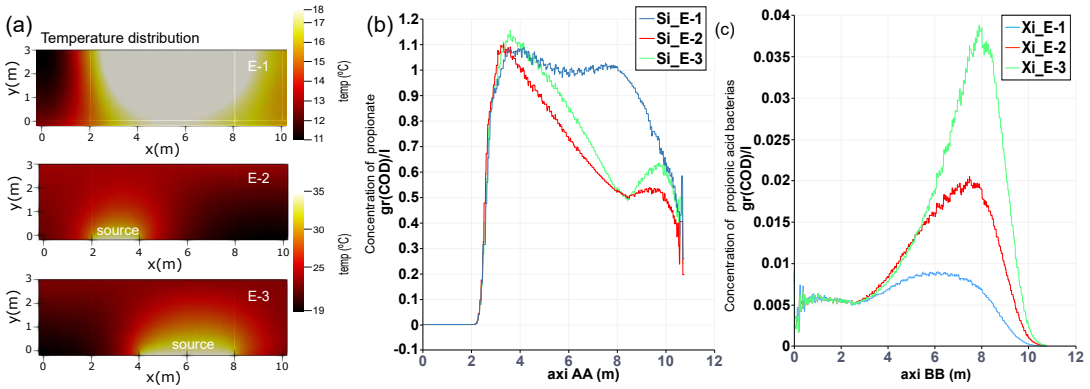

Figure 6. (**a**) Temperature distribution under three different scenarios; E-1 Ambient temperature, E-2 includes a heat source at the bottom of the lagoon, between coordinates 2 and 4, and the E-3 between 4 and 8, in the x axis. (**b**,**c**) Concentration of propionate and cells, respectively, along the axis AA (see Figure 5) for the different scenarios detailed in (**a**).

The distribution of temperature is showed in Figures 3 and 6. As expected, the removal efficiency is improved by the rising temperature of the heat source, as is observed in the cases 2 and 3. However, this graphic also shows that organic matter is eliminated more efficiently in case 2 than in 3 in a percentage of 10 %. Consequently a minor residual concentration in the outlet pipe is achieved.

Table 5 sums up the propionate removal information for the four examples above mentioned. It shows the source and effluent concentrations, as well as the percentage removed. Best values correspond with case 4.

Table 5. Values of propionate concentrations and the rate per 100 removed.

Case	Source Si (mg(COD)/L)	Effluent Si (mg(COD)/L)	Removed (mg(COD)/L)	Percentage Removed
1	1500	280	1220	81.33%
2	1500	265	1235	82.33%
3	1700	215	1485	87.35%
4	1400	135	1265	90.35%

By analysing the table, it can be said that the propionate concentration at the outlet of the lagoon, once acetogenic bacteria have removed a great part of substrate in the system, is among 280 and 135 $mg \cdot L^{-1}$. By placing a heat source, strategically, at the bottom of the lagoon (E-2 and E-3) it is possible to reduce substrate concentrations at its outlet.

4. Conclusions

In this paper, we have proposed and assessed a methodology for anaerobic cells performance for wastewater treatment, in AL, under the influence of the temperature. It has been studied in terms of biomass and substrate concentrations. The model couples a series of PDEs, related to the phenomena associated to AL (ADRE, ADM1, Stokes and heat transfer), to each other.

Diffusion for horizontal and vertical directions, the movement of the bulk of the concentrations in accordance with a gradient, external temperature interactions, biochemical and physical–chemical reactions, and a set of boundary values were considered in this study.

This model builds understanding for microbial community's behaviour along the lagoon as a function of the temperature. Applying heat load in different points of the system, it has been possible to establish correlations through the graphics, as well as the comparison between diverse scenarios according to their corresponding boundary values. The results give us the possibility to obtain effective designs adapted to each circumstance, avoiding energy loss.

This methodology allows the optimization of unstirred flow systems, taking into account that the advantages of these systems make them more suitable for specific applications. The model can be used in the prediction of the effluent quality and in the design of AL to achieve better performances.

In view of the results, it can be concluded that this methodology has significant potential as a tool for both the design of AL, and the interactive learning of the microbial ecology in plug flow systems.

Supplementary Materials: The following are available online at https://www.mdpi.com/2073-4441/13/7/882/s1, Table S1: Biochemical rate coefficients and kinetic rate equations for soluble components. Table S2: Biochemical rate coefficients and kinetic rate equations for particulate components. Table S3: Dynamic state variables include in the stoichiometry matrix (Tables S1 and S2).

Author Contributions: Conceptualization, S.B.-E., A.R.-M., C.M.-P., S.O.P.-B. and F.L.-Z.; methodology, S.B.-E., S.O.P.-B. and A.R.-M.; software, S.B.-E. and A.R.-M.; formal analysis, S.B.-E. and A.R.-M.; investigation, S.B.-E., A.R.-M. and S.P.; resources, S.B.-E., A.R.-M., S.O.P.-B., C.M.-P. and F.L.; data curation, S.B.-E. and A.R.-M.; writing—original draft preparation, S.B.-E. and A.R.-M.; writing—review and editing, S.B.-E., and A.R.-M.; visualization, S.B.-E. and A.R.-M.; supervision, S.O.P.-B., C.M., F.L.-Z. and A.R.-M.; project administration, C.M.-P. and A.R.-M.; funding acquisition, S.O.P.-B. and A.R.-M. All authors have read and agreed to the published version of the manuscript.

Funding: This research was co-funded by the INTERREG V-A Cooperation, Spain-Portugal MAC (Madeira-Azores-Canarias) 2014–2020 pro-gramme, MITIMAC project (MAC2/1.1a/263).

Institutional Review Board Statement: Not applicable.

Informed Consent Statement: Not applicable.

Data Availability Statement: Not applicable.

Acknowledgments: This research has been co-funded by the INTERREG V-A Cooperation, Spain-Portugal MAC (Madeira-Azores-Canarias) 2014–2020 pro-gramme, MITIMAC project (MAC2/1.1a/263).

Conflicts of Interest: The authors declare no conflict of interest.

Abbreviations

The following abbreviations are used in this manuscript:

ADM1	Anaerobic Digestion Model No1
IWA	International Water Association
AD	Anaerobic Digestion
AL	Anaerobic Lagoons
FEM	Finite element method
CFD	Computational fluid dynamic
PDE	Partial differential equation
ADRE	Advection–diffusion-reaction equation

Nomenclature

The following nomenclature are used in this manuscript

Δ	Laplace operator $\Rightarrow \Delta = \frac{\partial^2}{\partial x_i^2}$
∇	Gradient operator $\Rightarrow \nabla = \frac{\partial}{\partial x_i}$
Ω_r	Reactor (lagoon) domain
Ω_g	Ground domain surrounding the lagoon
$\mathbb{H}_0^1, \mathbb{P}_0^1, \mathbb{P}_0^2$	Hilbert space
Γ_D	Dirichlet boundary condition
Γ_N	Neumann boundary condition
Γ_R	Robin boundary condition
$\vec{v}, q, Y_i, W$	Smooth functions
$\mathfrak{D}$	Diffusive coefficient
μ_{max_i}	Maximum specific growth rate
$\vec{u}$	Velocity vector
ν	Viscosity
T	Temperature
$T_{a,ext}$	Temperature of the externally surrounding surface
T_{max}	Maximum growth-temperature
T_{min}	Minimum growth-temperature
T_{dp}	Dew-point temperature
T_{UGT}	Undisturbed ground temperature
T_{opt}	Temperature for maximum specific growth
T_{sky}	Sky radiative temperature
G	Irradiance
RH	Average relative humidity
σ	Stefan-Boltzmann constant
ε	Emissivity
h_{int}	Internal convective heat transfer coefficient
k_i	Heat conductivity for Ω_i, where i = 1,2,3. ..
n	Unit normal
Θ	Angle between the beam direction and the normal to the surface
μ_{opt}	Optimal value of the maximum specific growth rate
I_i	Inhibition coefficient
Kd	Specific microorganism decay rate
ρ_j	Kinetic rate of process j
K_{S_1}	Substrate saturation constant
S_i	Substrate concentrations
Y_1	Substrate yield coefficient
X_i	Biomass concentration
ϕ	Scalar field
p	Pressure
ρ_0	Density
Q	Flow
t	Time

Appendix A

Table A1. Cardinal temperature and maximum specific growth rate at the optimal temperature for representative cells of the different phases in the anaerobic digestion [10,39,40].

Process	T_{min}(°C)	T_{op}(°C)	T_{max}(°C)	$\mu_{opt}(hr-1)$
Hydrolysis/acidogenesis	11	39.3	45.8	1.1
Acetogenesis	5.6	40.3	47.3	1.4
Methanogenesis	11.1	34.1	46.3	1.1

References

1. Parralejo, A.; Royano, L.; González, J.; González, J. Small scale biogas production with animal excrement and agricultural residues. *Ind. Crops Prod.* **2019**, *131*, 307–314. [CrossRef]
2. Holm-Nielsen, J.; Seadi, T.A.; Oleskowicz-Popiel, P. The future of anaerobic digestion and biogas utilization. *Bioresour. Technol.* **2009**, *100*, 5478–5484. [CrossRef]
3. Park, J.H.; Park, J.H.; Lee, S.H.; Jung, S.P.; Kim, S.H. Enhancing anaerobic digestion for rural wastewater treatment with granular activated carbon (GAC) supplementation. *Bioresour. Technol.* **2020**, *315*, 123890. [CrossRef] [PubMed]
4. Jiang, Y.; Bebee, B.; Mendoza, A.; Robinson, A.K.; Zhang, X.; Rosso, D. Energy footprint and carbon emission reduction using off-the-grid solar-powered mixing for lagoon treatment. *J. Environ. Manag.* **2018**, *205*, 125–133. [CrossRef] [PubMed]
5. Duan, N.; Zhang, D.; Khoshnevisan, B.; Kougias, P.G.; Treu, L.; Liu, Z.; Lin, C.; Liu, H.; Zhang, Y.; Angelidaki, I. Human waste anaerobic digestion as a promising low-carbon strategy: Operating performance, microbial dynamics and environmental footprint. *J. Clean. Prod.* **2020**, *256*, 120414. [CrossRef]
6. Mendieta-Pino, C.A.; Ramos-Martin, A.; Perez-Baez, S.O.; Brito-Espino, S. Management of slurry in Gran Canaria Island with full-scale natural treatment systems for wastewater (NTSW). One year experience in livestock farms. *J. Environ. Manag.* **2019**, *232*, 666–678. [CrossRef]
7. Muga, H.; Mihelcic, J. Sustainability of wastewater treatment technologies. *J. Environ. Manag.* **2008**, *88*, 437–447. [CrossRef]
8. Wu, B.; Chen, Z. An integrated physical and biological model for anaerobic lagoons. *Bioresour. Technol.* **2011**, *102*, 5032–5038. [CrossRef]
9. Wu, B. Advances in the use of CFD to characterize, design and optimize bioenergy systems. *Comput. Electron. Agric.* **2013**, *93*, 195–208. [CrossRef]
10. Donoso-Bravo, A.; Sadino-Riquelme, C.; Gómez, D.; Segura, C.; Valdebenito, E.; Hansen, F. Modelling of an anaerobic plug-flow reactor. Process analysis and evaluation approaches with non-ideal mixing considerations. *Bioresour. Technol.* **2018**, *260*, 95–104. [CrossRef]
11. Rajeshwari, K.; Balakrishnan, M.; Kansal, A.; Lata, K.; Kishore, V. State-of-the-art of anaerobic digestion technology for industrial wastewater treatment. *Renew. Sustain. Energy Rev.* **2000**, *4*, 135–156. [CrossRef]
12. Lauwers, J.; Appels, L.; Thompson, I.P.; Degrève, J.; Impe, J.F.V.; Dewil, R. Mathematical modelling of anaerobic digestion of biomass and waste: Power and limitations. *Prog. Energy Combust.* **2013**, *39*, 383–402. [CrossRef]
13. Wade, M.; Harmand, J.; Benyahia, B.; Bouchez, T.; Chaillou, S.; Cloez, B. Perspectives in mathematical modelling for microbial ecology. *Ecol. Model.* **2016**, *321*, 64–74. [CrossRef]
14. Batstone, D.; Keller, J.; Angelidaki, I.; Kalyuzhnyi, S.; Pavlostathis, S.; Rozzi, A.; Sanders, W.; Siegrist, H.; Vavilin, V. The IWA Anaerobic Digestion Model No 1 (ADM1). *Water Sci. Technol.* **2002**, *45*, 65–73. Available online: http://xxx.lanl.gov/abs/http://wst.iwaponline.com/content/45/10/65.full.pdf (accessed on 1 september 2020). [CrossRef] [PubMed]
15. Kleerebezem, R.; van Loosdrecht, M.C.M. Critical analysis of some concepts proposed in ADM1. *Water Sci. Technol.* **2006**, *54*, 51–57. [CrossRef]
16. Li, D.; Lee, I.; Kim, H. Application of the linearized ADM1 (LADM) to lab-scale anaerobic digestion system. *J. Environ. Chem. Eng.* **2021**, *9*, 105193. [CrossRef]
17. Fleming, J.G. Novel Simulation of Anaerobic Digestion Using Computational Fluid Dynamics. Ph.D. Thesis, North Carolina State University, Raleigh, NC, USA, 2002.
18. Goodarzi, D.; Sookhak Lari, K.; Mossaiby, F. Thermal effects on the hydraulic performance of sedimentation ponds. *J. Water Process. Eng.* **2020**, *33*, 101100. [CrossRef]
19. Brito-Espino, S.; Ramos-Martín, A.; Pérez-Báez, S.; Mendieta-Pino, C. Application of a mathematical model to predict simultaneous reactions in anaerobic plug-flow reactors as a primary treatment for constructed wetlands. *Sci. Total Environ.* **2020**, *713*, 136244. [CrossRef] [PubMed]
20. Mahmudul, H.; Rasul, M.; Akbar, D.; Narayanan, R.; Mofijur, M. A comprehensive review of the recent development and challenges of a solar-assisted biodigester system. *Sci. Total Environ.* **2021**, *753*, 141920. [CrossRef]
21. Atelge, M.; Atabani, A.; Banu, J.R.; Krisa, D.; Kaya, M.; Eskicioglu, C.; Kumar, G.; Lee, C.; Yildiz, Y.; Unalan, S.; et al. A critical review of pretreatment technologies to enhance anaerobic digestion and energy recovery. *Fuel* **2020**, *270*, 117494. [CrossRef]

22. Tumilar, A.S.; Milani, D.; Cohn, Z.; Florin, N.; Abbas, A. A Modelling Framework for the Conceptual Design of Low-Emission Eco-Industrial Parks in the Circular Economy: A Case for Algae-Centered Business Consortia. *Water* **2021**, *13*, 69. [CrossRef]
23. Haßler, S.; Ranno, A.M.; Behr, M. Finite-element formulation for advection–reaction equations with change of variable and discontinuity capturing. *Comput. Methods Appl. Mech. Eng.* **2020**, *369*, 113171. [CrossRef]
24. Mirza, I.A.; Akram, M.S.; Shah, N.A.; Imtiaz, W.; Chung, J.D. Analytical solutions to the advection-diffusion equation with Atangana-Baleanu time-fractional derivative and a concentrated loading. *Alex. Eng. J.* **2021**, *60*, 1199–1208. [CrossRef]
25. Singh, S.; Bansal, D.; Kaur, G.; Sircar, S. Implicit-explicit-compact methods for advection diffusion reaction equations. *Comput. Fluids* **2020**, *212*, 104709. [CrossRef]
26. Zeng, L.; Chen, G. Ecological degradation and hydraulic dispersion of contaminant in wetland. *Ecol. Model.* **2011**, *222*, 293–300. [CrossRef]
27. Bozkurt, S.; Moreno, L.; Neretnieks, I. Long-term processes in waste deposits. *Sci. Total Environ.* **2000**, *250*, 101–121. [CrossRef]
28. Song, L.; Li, P.W.; Gu, Y.; Fan, C.M. Generalized finite difference method for solving stationary 2D and 3D Stokes equations with a mixed boundary condition. *Comput. Math. Appl.* **2020**, *80*, 1726–1743. [CrossRef]
29. Ukai, S. A solution formula for the Stokes equation in Rn+. *Commun. Pure Appl. Math.* **1987**, *40*, 611–621. [CrossRef]
30. Reddy, J.; Gartling, D. *The Finite Element Method in Heat Transfer and Fluid Dynamics*, 3rd ed.; CRC Press: Boca Raton, FL, USA, 2010; pp. 1–483.
31. Alvarez-Hostos, J.C.; Bencomo, A.D.; Puchi-Cabrera, E.S.; Fachinotti, V.D.; Tourn, B.; Salazar-Bove, J.C. Implementation of a standard stream-upwind stabilization scheme in the element-free Galerkin based solution of advection-dominated heat transfer problems during solidification in direct chill casting processes. *Eng. Anal. Bound. Elem.* **2019**, *106*, 170–181. [CrossRef]
32. Guldentops, G.; Van Dessel, S. A numerical and experimental study of a cellular passive solar façade system for building thermal control. *Sol. Energy* **2017**, *149*, 102–113. [CrossRef]
33. Lawrence, M.G. The Relationship between Relative Humidity and the Dewpoint Temperature in Moist Air: A Simple Conversion and Applications. *Bull. Am. Meteorol. Soc.* **2005**, *86*, 225–234. [CrossRef]
34. Çengel, Y. Heat Transfer: A Practical Approach. In *McGraw-Hill Series in Mechanical Engineering*; McGraw Hill Books: London, UK, 2003.
35. Walton, G.N. *Thermal Analysis Research Program Reference Manual*; NBSIR, Department of Energy, Office of Building Energy Research and Development: Washington, DC, USA, 1983.
36. Monod, J. The Growth of Bacterial Cultures. *Annu. Rev. Microbiol.* **1949**, *3*, 371–394. [CrossRef]
37. Rosso, L.; Lobry, J.; Flandrois, J. An Unexpected Correlation between Cardinal Temperatures of Microbial Growth Highlighted by a New Model. *J. Theor. Biol.* **1993**, *162*, 447–463. [CrossRef]
38. Herus, V.A.; Ivanchuk, N.V.; Martyniuk, P.M. A System Approach to Mathematical and Computer Modeling of Geomigration Processes Using Freefem++ and Parallelization of Computations. *Cybern Syst. Anal.* **2018**, *54*, 284–292. [CrossRef]
39. Donoso-Bravo, A.; Bandara, W.; Satoh, H.; Ruiz-Filippi, G. Explicit temperature-based model for anaerobic digestion: Application in domestic wastewater treatment in a UASB reactor. *Bioresour. Technol.* **2013**, *133*, 437–442. [CrossRef] [PubMed]
40. Donoso-Bravo, A.; Retamal, C.; Carballa, M.; Ruiz-Filippi, G.; Chamy, R. Influence of temperature on the hydrolysis, acidogenesis and methanogenesis in mesophilic anaerobic digestion: Parameter identification and modeling application. *Water Sci. Technol.* **2009**, *60*, 9–17. [CrossRef] [PubMed]

Interreg
water
MAC 2014-2020
Cooperación Territorial
MITIMAC
MITIGACIÓN DEL CAMBIO CLIMÁTICO A TRAVÉS DE LA INNOVACIÓN EN EL CICLO DEL AGUA MEDIANTE TECNOLOGÍAS BAJAS EN CARBONO
MDPI

Article

Proposal of a Laboratory-Scale Anaerobic Biodigester for Introducing the Monitoring and Sensing Techniques, as a Potential Learning Tool in the Fields of Carbon Foot-Print Reduction and Climate Change Mitigation

Saulo Brito-Espino [1], Federico Leon [1,*], Jenifer Vaswani-Reboso [1], Alejandro Ramos-Martin [2] and Carlos Mendieta-Pino [1]

[1] Institute of Environmental Studies and Resources (IUNAT), Campus Tafira, University of Las Palmas de Gran Canaria, 35017 Las Palmas de Gran Canaria, Spain; saulobrito09@gmail.com (S.B.-E.); jenifer.vaswani@ulpgc.es (J.V.-R.); carlos.mendieta@ulpgc.es (C.M.-P.)
[2] Departament of Process Engineering, Campus Tafira, University of Las Palmas de Gran Canaria, 35017 Las Palmas de Gran Canaria, Spain; alejandro.ramos@ulpgc.es
* Correspondence: federicoleon@perezvera.com; Tel.:+34-6861-69516

Abstract: This article presents a proposal of an anaerobic biodigester on a laboratory scale for introducing the monitoring and sensing techniques of the growth of microorganisms according to different parameters, where the redox potential, pH, pressure, and temperature have been measured in quasi-continuous mode. For this task, a microcontroller system was used (Atmega328—Arduino). Importantly, the design is based on flexible and open-source software, hardware, and firmware (Scilab, Arduino, Processing), facilitating its modification for other related studies. This design was developed to help engineering students to learn and to understand the operation of an anaerobic biodigester, which allows us to know various properties of the system at any time, as well as its evolution over time. In this way, property curves can be drawn and related to each other to obtain a better understanding of the biodigester operation. In this context, the relationship between the oxide-reduction reaction and microbial activity was studied so that the redox potential can be a way of measuring the growth of microorganisms in an anaerobic environment. With all this, through these parameters, it is possible to introduce to engineering students the operation of this technology used normally like a very powerful tool for the control of the carbon footprint, for example in wastewater sector, and consequently for the mitigation of the climate change.

Keywords: wastewater; low-carbon; biodigester; laboratory scale; open-source tools

Citation: Brito-Espino, S.; Leon, F.; Vaswani-Reboso, J.; Ramos-Martin, A.; Mendieta-Pino, C. Proposal of a Laboratory-Scale Anaerobic Biodigester for Introducing the Monitoring and Sensing Techniques, as a Potential Learning Tool in the Fields of Carbon Foot-Print Reduction and Climate Change Mitigation. *Water* **2021**, *13*, 2409. https://doi.org/10.3390/w13172409

Academic Editor: Hongyu Ren

Received: 4 August 2021
Accepted: 29 August 2021
Published: 1 September 2021

1. Introduction

Anaerobic digestion technologies, applied to organic water treatment, are efficient ways to solve environmental problems also provide energy. They are considered sustainable, safe, and efficient biotechnologies in which carbon footprint reduction, by CH_4 capture and fossil fuel replacement, is clearly a factor to take under advisement [1–7]. The process of anaerobic digestion has been known and applied since ancient times; however, it was understood in terms of its final products and not its processes [3]. The versatility of anaerobic digestion applied as an effective technology in the face of certain fundamental challenges has found its usefulness in biotechnological industries [4–7]. Unlike aerobic processes where dissolved oxygen can be measured continuously, there is a great challenge for fermentative processes in anaerobic organisms where the technologies referring to control processes are currently insufficient [6–10]. Since pH detection has been commonly used in fermentation processes, where only the activity of the proton is reflected, it is not sensitive to small changes in the intracellular metabolism. The redox potential (ORP) known as

oxidation-reduction or oxide-reduction potential, reflects all the electrons transferred and reflects the intracellular metabolism [6,11–15].

Recent advances in analytical technologies allow complex bioconversion processes to be controlled and deciphered. Few parameters in this process are routinely recorded continuously and immediately, such as pH, ORP, gas production rate, and flow rates [16–19].

Within this context, and due to the great number of applications that are being given to the anaerobic biodigesters, that is why it would be necessary to develop a strategy so that the engineering students could understand and develop its operation as well as the parameters that govern it, all applied to different situations. The learning of these strategies could be achieved using this equipment or through experimental designs carried out by students. This educational proposal is based on theoretical psychological studies published in numerous articles [5,7,8,20–24] which emphasize that students can reinforce their learning through an appropriate teaching environment, as well as through the use, construction, and design of equipment.

After describing the importance of the anaerobic process and the consequent need to control it, at all times, the decision was taken to present the design and manufacture of an anaerobic batch biodigester on a laboratory scale, as well as its implementation through a practical application in which brewer's yeast (Saccharomyces cerevisiae) was introduced, and it was subjected to a semi-continuous control process, the results of which were subsequently compared with a previously proposed theoretical model [25–30].

The main objective of this article is to show an experimental design at laboratory scale of an anaerobic biodigester. In the same way, a series of tools, software, and hardware are proposed, which are easy to use and of low cost, and which will allow engineering students to see that they can develop autonomous elements to control an element, as well as to transform the information received into parameters that can later be interpreted in a computer [31–34]. The specific objective of this research is to relate the process of anaerobic digestion in a sequentially loaded reactor on a laboratory scale for a known microorganism and with a substrate prepared in the laboratory, to the profiles of oxidation-reduction potential, pH, temperature, and absolute pressure [35–39].

2. Materials and Methods

2.1. Diagram of the Laboratory Reactor

The designed bioreactor (Figure 1) can be grouped into three distinct parts: (1) Digestion system—which includes the digester itself, as well as those elements that are in direct contact with it (sensors, heating cable, loading, and unloading supply, etc.); (2) Control system, circuits, and voltage source—it receives data and sends the orders necessary for the proper functioning of the system; and (3) Computer system, communication interface and software [40–44].

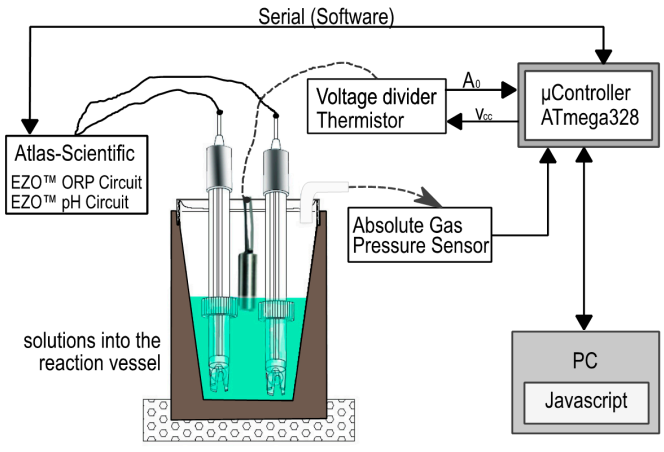

Figure 1. Basic diagram of experimental design.

2.1.1. Digestion System

It is made up of an insulated hermetic container, with a feeding and evacuation system arranged so that the mixture is guaranteed in each loading and unloading process. The upper part of the container has a series of sensors that are defined below:

- pH Sensor: Scientific Grade Silver/Silver Chloride pH), 10 sensor with a response speed of 95% in one second.
- ORP sensor, (E): High quality sensor from Atlas Scientific [10,45–48]. The data transmission mode is through an integrated system and with a simple serial communication protocol which gives us an immediate response of the E value.
- Absolute Pressure Sensor: Phidgets mod. 1141-0—Absolute Sensor of gas pressure from 15 to 115 kPa [49,50]. This is a high-level sensor with analogue input, with input proportional to the of the environment. The pressure measurement for this sensor is 15 kPa. The formula used to translate the sensor value into pressure was the following [2,51,52]:

$$\text{Pressure (kPa)} = (\text{Sensor Value}/9.2) + 10. \quad (1)$$

- Temperature sensor: Two miniature Vishay NTC thermistors (Figure 2) were used to take external and internal temperature readings. Their main characteristics are described in Table 1.

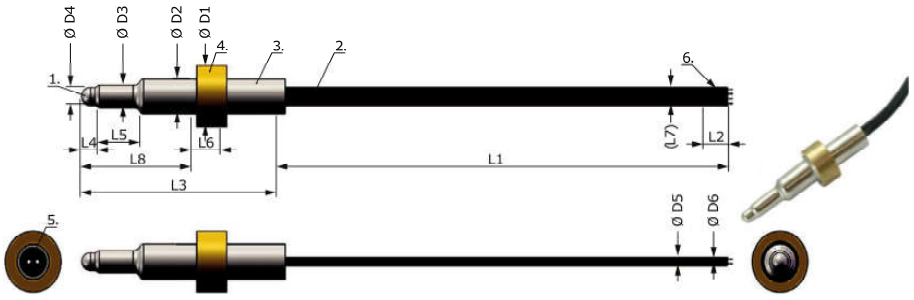

L1	L2	L3	L4	L5	L6	L7	L8	Ø D1	Ø D2	Ø D3	Ø D4	Ø D5	Ø D6
200 ± 20	4 ± 1	23 ± 0.5	2 ± 0.5	5 ± 0.5	3.4 ± 0.2	2.05	13 ± 0.5	6.8 ± 0.1	3.9 ± 0.1	2.5 ± 0.2	2 ± 0.2	1	0.3

Figure 2. Thermistor NTC Vishay, dimensions in millimeters.

For the calculation of the temperature from the analogical measurement, considering the resistive values depending on the temperature provided by the manufacturer, and with an algorithm in Scilab, we obtain Equation (2).

$$f(x) = 2.249 \times 10^{-5}x^2 + 0.06872x - 16.03 \quad (2)$$

Table 1. Characteristics of the thermistor NTC, Vishay.

Parameter	Value	Units
Resistence value at 25 °C	10 K	Ω
Tolerance of R25	±3	%
B25/85 (Beta)	3984	K
Temperatura range of operation	−25 to 105	°C

2.1.2. Circuits and Control System

Arduino Uno (Figure 3) microcontroller model ATmega328 (Atmel) was implemented within an embedded system in order to control the measuring processes providing bidirectional communication with the circuit of the electrical conductivity probe, transferring the respective data to the PC via USB for archival purposes.

Figure 3. Arduino Uno.

Figures 4 and 5 show the general circuit diagram and pictures where all the elements necessary for the correct operation of the system are collected, as well as the data collection to be processed later. It is composed of a voltage source of 12 V that feeds: the transistor, a heat source, thermistors and a stirring system, a microcontroller hard plate, a PWM plate through which the bioreactor temperature is controlled by a transistor, a plate for the temperature sensors, auxiliary connection plates and sensor plates, resistors, diodes, and wiring.

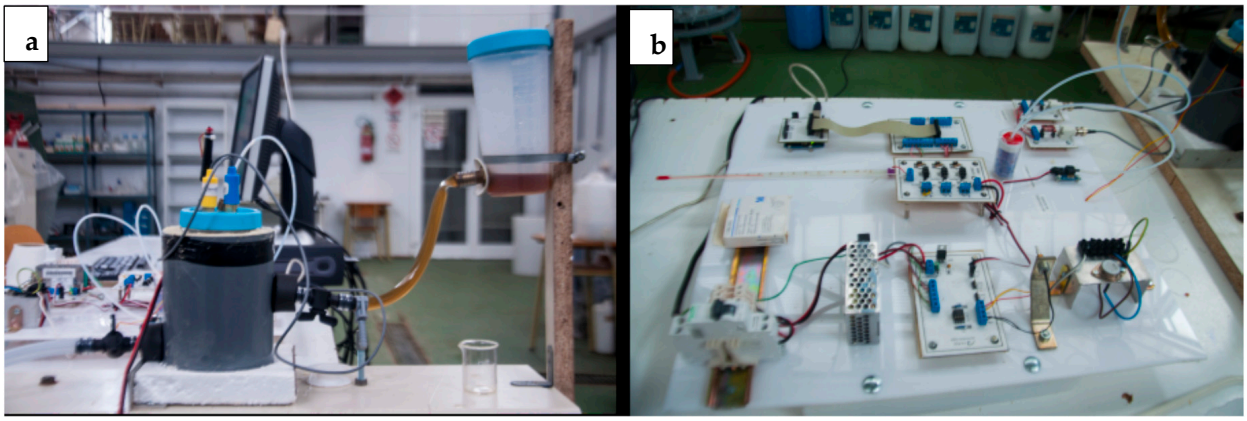

Figure 4. Photos of the reactor and sensors (**a**) and the circuits with the controls systems (**b**).

2.1.3. Computer System, Communication Interface, and Software

As for the computer system, a data transmission source code was developed for the pH, E, pressure, and temperature sensors with Processing software (source code in Appendix C). The output data was transferred to the Arduino ide serial monitor for checking and control, and then through the Processing software interface for saving into file the sensor samplings.

2.1.4. Auxiliary Equipment and Laboratory Material

The auxiliary equipment were the following: an Atago RX-7000 Alfa3 refractometer used for the effluent measurements, the refraction product, and the Brix degrees (°Bx); and precision weights. As far as materials are concerned, all those related to the sampling and measurement of volumes (typical of a laboratory) were used, such as flasks, pipettes, spoons, etc.

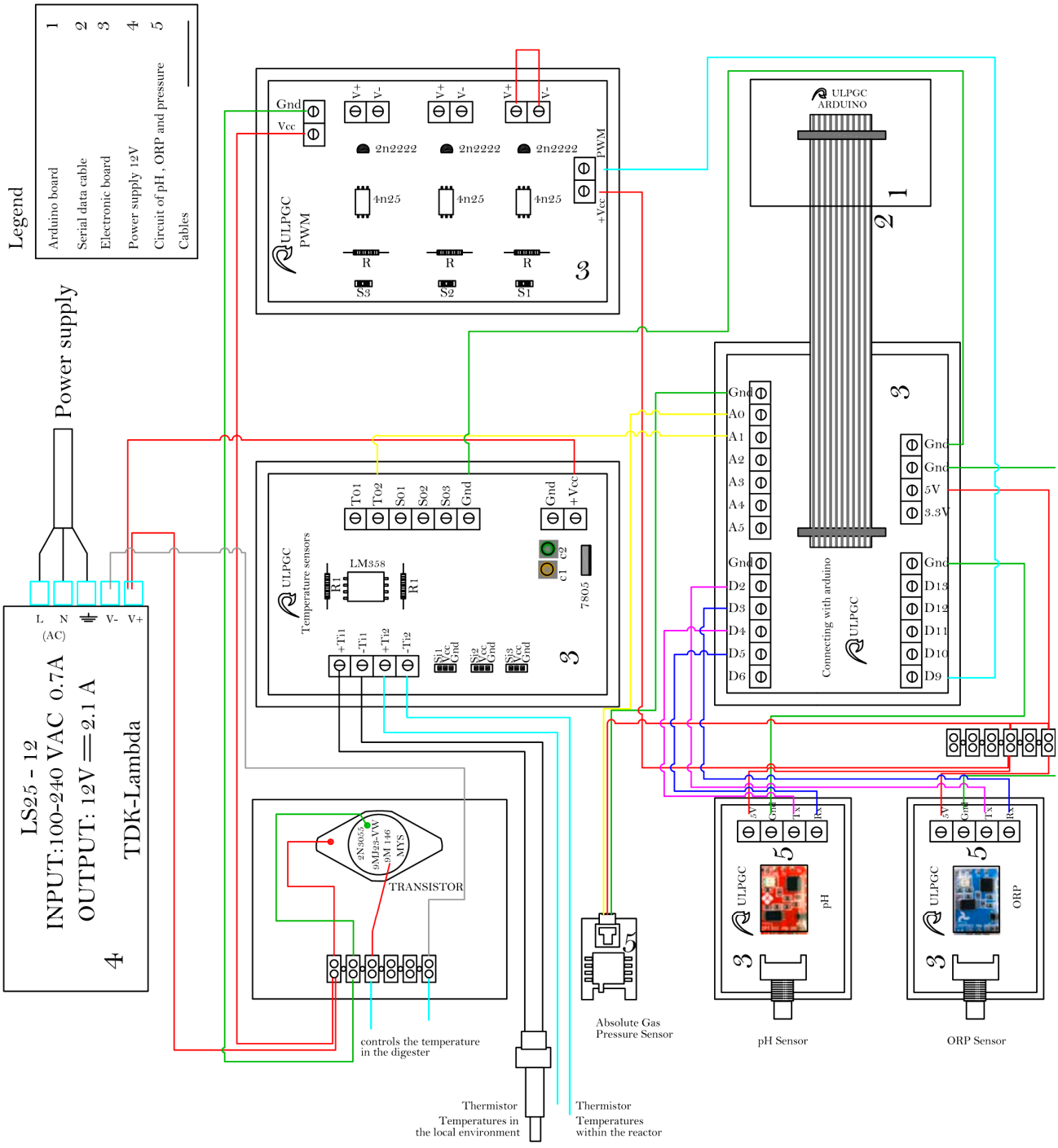

Figure 5. Circuits and control system design.

2.2. Preparation and Testing

2.2.1. Preparation of the Substrate

For the preparation of the substrate, the procedure described in bibliography was followed [4]. (1) The substrate was prepared, and its suitability checked. (2) The Brix level was measured and verified to be between 17 and 20 degrees. (3) Once this process was finished, 200 mL of the must was taken, and the yeast was added to it (approximately 2–4 g/L). Although an activation temperature of 37 °C is normally required, it was left at room temperature, as it has been previously proven that the inoculum is active under these conditions for working yeast.

2.2.2. Microbial Inoculum

Brewer's yeast was used whose species includes Saccharomyces cerevisiae with a yield of 0.25–0.33 kg of dry cell weight per kg of substrate.

2.2.3. Control and Saving Data

Through the Arduino (Appendix B shows the Arduino source code), the temperature was controlled and the signals from the pH, ORP, absolute pressure, and temperature sensors (inside the digester and outside the environment) were read. Data were sent to the computer where they were stored by means of the use of Processing tool. Shown in Appendix C is the Processing source code, and Figure 6 displays the interface. Once all the information was entered, it was saved in a file on the computer's hard disk.

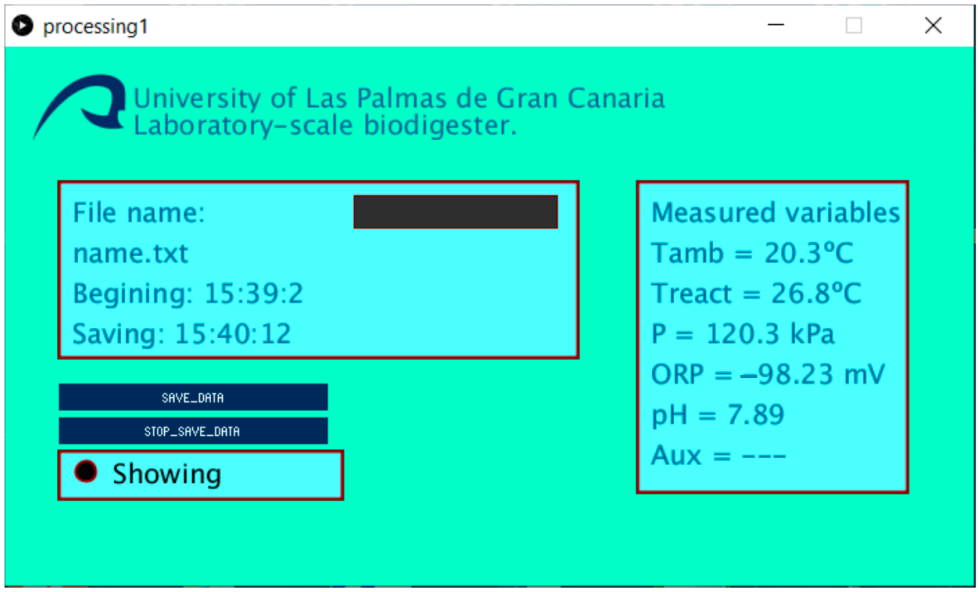

Figure 6. Processing PC interface data logger.

3. Results

3.1. Digestion Model

Dynamic simulation between reality and model is a very important way for research, as it enables to provide strategies for the digester operation. In the model, the description of all metabolic rates is based on the classical Monod equation,

$$\mu = \mu_{max} \frac{S}{K_s + S}$$

where μ is the growth rate of a considered biomass, μ_{max} is the maximum growth rate of this microorganism, S is the concentration of the limiting substrate S for growth, K_s is the half-velocity constant for the substrate S when $\frac{\mu}{\mu_{max}} = 0.5$.

The matrix differential equation related to biomass and substrate dynamic is as follows:

$$\frac{dX}{dt} = \left(\mu_{max} \frac{S}{K_s + S}\right) X$$

$$\frac{dS}{dt} = \left(\beta_s \mu_{max} \frac{S}{K_s + S}\right) X$$

where S and X are the substrate and biomass concentration respectively, β_s is the stoichiometric ratio for S.

Figure 7 shows a simulation with discontinuous dynamics (Scilab source code in Appendix A) with period T = 24 h. Both the evolution of the substrate and that of the biomass, as can be seen in the system, start from an initial state and, after the transitory process, reach a stationary state.

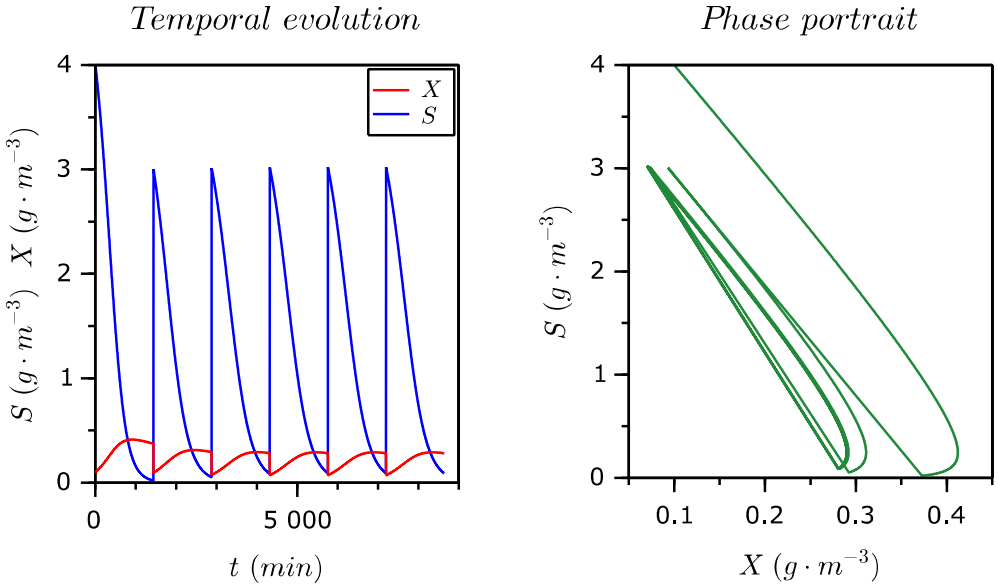

Figure 7. Concentration of biomass and substrate where $\mu_{max} = 0.75\ (h^{-1})$, $K_s = 10$, $\beta_s = 1.8$, $X_{(t=0)}$ is 0.1 (g/m^3) and $S_{(t=0)}$ is 4 (g/m^3).

3.2. Anaerobic Digester Start-Up and Operation

An average representation of the tests, carried out in the biodigester over 5 weeks, is shown in Table 2. The data was processed using a computerised tool from Scilab. Scilab is a software for numerical analysis, with a high-level programming language for scientific calculation. With the obtained data, a series of graphs were elaborated and the most relevant ones are presented in Figures 8–10.

Table 2. Laboratory-scale biodigester; performance periods, operating volume, and Brix measures.

Stage	Date	Feeding/Evacuation	Brix Grades			Remarks
		(mL)	1st Lecture	2nd Lecture	Average	
1	13 June	300	20.30		20.30	
2	18 June	75	20.31	20.29	20.30	
3	23 June	50	20.33	20.24	20.26	Addition NaOH (↑alkalinity)

The expression of the oxidation-reduction reactions can be expressed by the Nernst Equation (3).

$$E = E^0 + \frac{2.303RT}{nF} log_{10}\left(\frac{\text{Product of activities of oxidized species}}{\text{Product of reduced species activities}}\right) \quad (3)$$

where E^0 is the standard ORP, n is the number of exchanged electrons, and F is the Faraday constant (96.42 kJ/g equivalent volts).

The three periods from Table 2 are represented in the graphs as they are the most illustrative. It had taken a time of 1–3000 min for each of them.

3.2.1. First Stage

This stage includes from the start-up of the bioreactor to the first charge/discharge process. Figure 8 shows the ORP, pH, and temperature versus the time, in minutes. The

pH profile remains stable with adequate value for fermentative processes, around 4.4, with slight oscillations, while the ORP values indicate, practically, reducing conditions, in a slightly wider range that the previous one. This last achieves its maximum value, 100 (mV), at 1000 min, and minimum value, −250 mV at 1300 min; however, it tends to stabilize with fermentation time. This performance is reflected as well in other works [53,54]. On the other hand, during the whole of this period, temperature moved between 23.6 and 24.6 °C. It is observable that for high value of temperature, the ORP 's graph tends to drop.

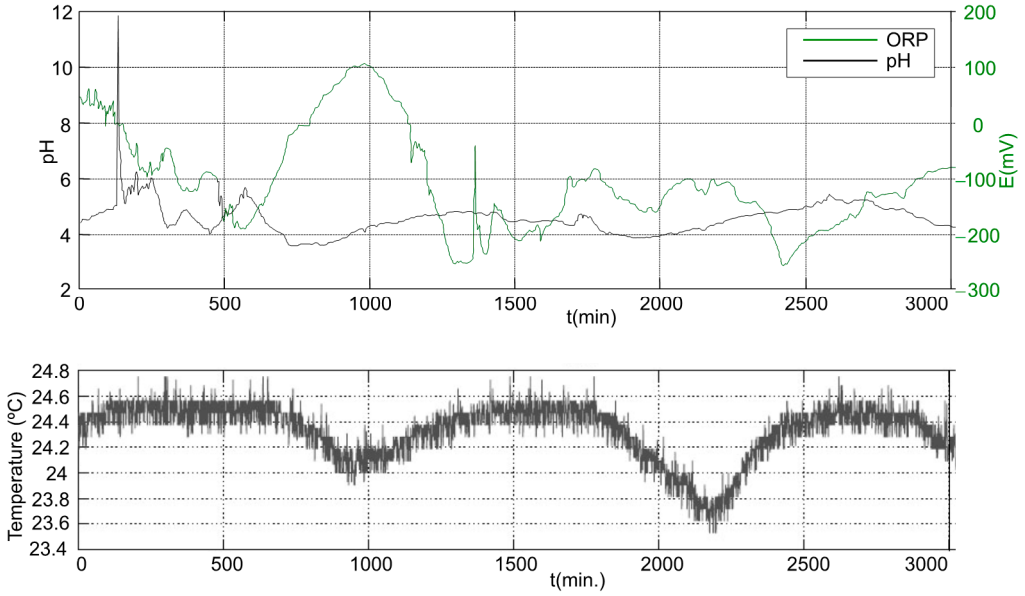

Figure 8. ORP, pH, and temperature in the first period.

In general, the ORP graph shows a downward slope with a very irregular profile.

3.2.2. Second Stage

In this occasion, the system was fed back by 75 mL of a new mixing (see Table 2). From Figure 9, it is observed, in the first third of the stage, a sharp fall in ORP, −85 mV; it immediately increases until it reaches a maximum value, 40 mV, then it begins to decrease gradually. This may have occurred due to the supply of substrate indicating an increase in activity in the first third of the period recorded. The difference in feedstock could change the microbial community and dominant species in anaerobic digestion process. In relation to temperature, the ORP maintains the same vein as that in the previous case.

3.2.3. Third Stage

For this stage, the alkalinity in the reactor was increased by the adding NaOH mixed with the substrate in the follow feeding. The basic environment of the system reflects negative ORP values, between −300 and −470 mV. The graph, Figure 10, shows a gradual decreasing trend of ORP along this period. It is due to the buffering capacity of anaerobic digestion. Similar results have been achieved by other authors [55–58].

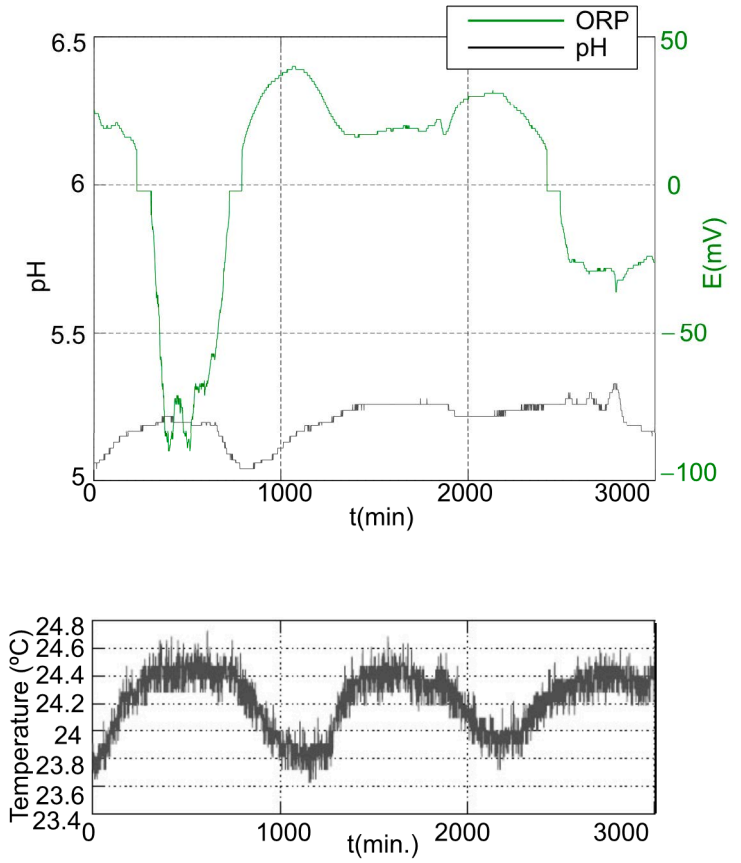

Figure 9. ORP, pH, and Temperature in the second period.

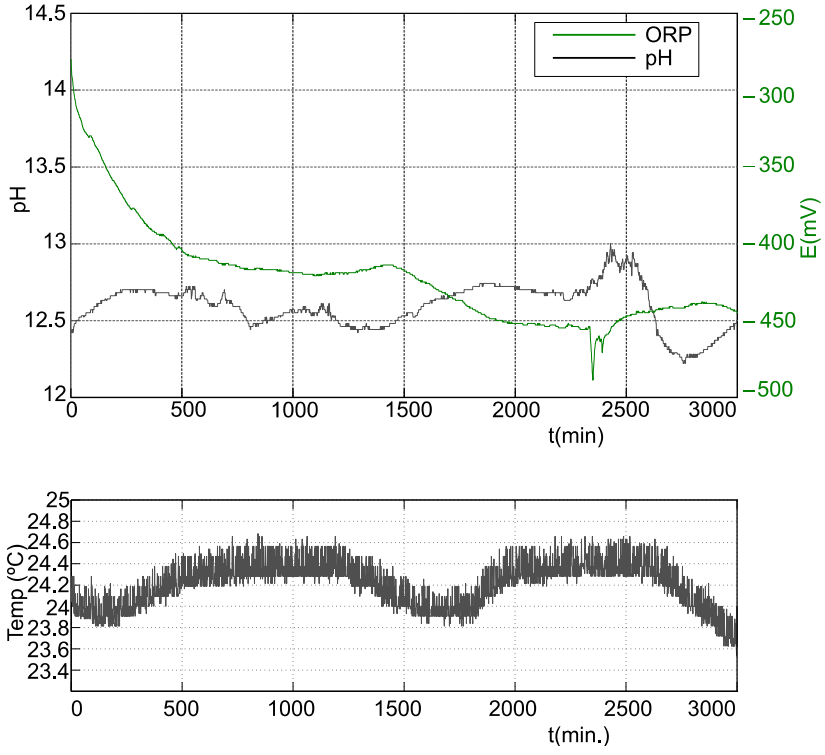

Figure 10. ORP, pH, and Temperature in the third period.

4. Conclusions

The proposed anaerobic biodigester monitored system works well, allowing for small-scale testing. Its use in research and teaching will allow the development of new research projects in the same way that it will help engineering students in their learning. With this design, it will be easy to determine the factors that can affect the growth of the anaerobic microorganism through the continuous data collection by the ORP, pH, temperature, and pressure sensors. Subsequently, with the subsequent processing of the data, it is possible to make graphs to be contrasted with a previously proposed theoretical model, and at the same time it can be compared with the equations that govern its behavior (Nernst equation).

On the other hand, this design has been supported by flexible and easily accessible free software, this being an important advantage for students since it offers the possibility of adapting this experimental design to each specific case, and the whole software used is free and open source.

The results show that the experimental design is feasible for the control and data collection of magnitudes related to the growth of an anaerobic bacteria in a digester.

Finally, it should be remembered that the design and construction of a laboratory-scale biodigester, due to its economic viability, is a tool available to engineering students for the development of their knowledge and learning.

Author Contributions: Conceptualization, S.B.-E. and A.R.-M.; methodology, S.B.-E. and A.R.-M.; software, S.B.-E. and A.R.-M.; validation, F.L., A.R.-M., S.B.-E., J.V.-R. and C.M.-P.; formal analysis, S.B.-E. and A.R.-M.; investigation, S.B.-E. and A.R.-M.; resources, A.R.-M. and J.V.-R.; data curation, F.L. and A.R.-M.; writing—original draft preparation, F.L. and A.R.-M.; writing—review and editing, F.L., C.M.-P. and J.V.-R.; visualization, S.B.-E., F.L. and A.R.-M.; supervision, F.L., C.M.-P., J.V.-R. and A.R.-M.; project administration, S.B.-E., F.L. and A.R.-M.; funding acquisition, J.V.-R., F.L. and A.R.-M. All authors have read and agreed to the published version of the manuscript.

Funding: This research received no external funding.

Institutional Review Board Statement: Not applicable for studies not involving humans or animals.

Informed Consent Statement: Informed consent was obtained from all subjects involved in the study.

Data Availability Statement: In this section, please provide details regarding where data supporting reported results can be found, including links to publicly archived datasets analyzed or generated during the study.

Acknowledgments: This research has been co-funded by the INTERREG V-A Cooperation Spain-Portugal MAC (Madeira-Azores-Canarias) programme MITIMAC project MAC2/1.1a/263.

Conflicts of Interest: The authors declare no conflict of interest.

Appendix A SCILAB Source Code

```
clear; clc;
mu_max=.1/3600;
k_s=100; k_d=.00001; k_x=.00000150;
V_1=.01; V_2=3.99; V_T=V_1+V_2;
S_min=k_d*k_s/(mu_max-k_d); S_in=130;
dt=100; time=200*24*3600; Delta_t=.05*24*3600;
q=round(Delta_t/dt);
t=0:dt:time;
X=zeros(1,length(t)); S=zeros(1,length(t));
X(1)=.1; S(1)=0; S_in=S_in; X_in=.1;
e=1; f=0; g=0;
for k=2:length(t)
```

```
        f=f+1;
        if f>=q //Impulse input
                S(k-1)=(V_2*S(k-1)+V_1*S_in)/V_T;
                X(k-1)=(V_2*X(k-1)+V_1*X_in)/V_T;
                f=0;
        end

        //Prediction step.
        X(k)=(1+(mu_max*S(k-1)/(k_s+S(k-1))-k_d)*dt)*X(k-1);
        S(k)=(1-k_x*X(k-1)/(k_s+S(k-1))*dt)*S(k-1);

        //Initialization and recursive correction steps.
        While (e>=.01)
                x=X(k);
                s=S(k);
                X(k)=X(k-1)+dt/2*((mu_max*S(k-1)/(k_s+S(k-1))-k_d)*X(k-1)+
        +(mu_max*S(k)/(k_s+S(k))-k_d)*X(k));
                S(k)=S(k-1)-k_x*dt/2*(S(k-1)/(k_s+S(k-1))*X(k-1)+S(k)/(k_s+S(k))*X(k));
                e=sqrt((x-X(k))^2+(s-S(k))^2);
        end
end
```

Appendix B Microcontroller Source Code (Arduino)

```
// *****Digital inputs for pH y ORP****
#include <SoftwareSerial.h> //add the soft serial libray
#define rxph 4 //set the RX pin to pin 2
#define txph 5 //set the TX pin to pin 3
#define rxorp 2#define txorp 3
// ****pH data***
SoftwareSerial phserial(rxph, txph); //enable the soft serial port
String inputstringph = ""; // string to hold incoming data from the PC
String sensorstringph = ""; //a string to hold the data from the Atlas Scientific product
boolean input_stringcompleteph = false;//have we received all the data from the PC
boolean sensor_stringcompleteph = false; //have we received all the data from the Atlas
Scientific product
// ****ORP data***
SoftwareSerial orpserial(rxorp, txorp);
String inputstringorp = ""; //a string to hold incoming data from the PC
String sensorstringorp = ""; //a string to hold the data from the Atlas Scientific product
boolean input_stringcompleteorp = false; //have we received all the data from the PC
boolean sensor_stringcompleteorp = false;//have we received all the data from the Atlas
Scientific product
// ****Analog inputs***
String sensorpresion="";//presion
float ntcbiodig=0; //termistor NTC lectura sistema de control
float ntcext=0; //termistor NTC lectura entorno
int analogPin1 = A1; //definimos los pines de entrada para la temperatura entorno
int analogPin2 = A2;//definimos los pines de entrada para la temperatura sistema
// **** SETUP ****
void setup(){ //set up the hardware

Serial.begin(9600);
```

```
phserial.begin(9600); //set baud rate for software serial port to 38400

orpserial.begin(9600);

phserial.print("r\r");

orpserial.print("r\r");

phserial.print("r\r");

orpserial.print("r\r");

inputstringph.reserve(5); //set aside some bytes for receiving data from the PC

sensorstringph.reserve(30); //set aside some bytes for receiving data from Atlas Scientific product

inputstringorp.reserve(5);//set aside some bytes for receiving data from the PC

sensorstringorp.reserve(30);

pinMode(analogPin1, INPUT); //def de los pines de entrada

pinMode(analogPin2, INPUT);
}
//**** loop ****

void loop(){
// ******Digital inputs *****

delay(60000);

input_stringcompleteph = true;

input_stringcompleteorp = true;

inputstringph="r\r";

inputstringorp="r\r";

bool mandar=true;


// ******pH*****

if (input_stringcompleteph){ //if a string from the PC has been recived in its entierty

phserial.print(inputstringph); //send that string to the Atlas Scientific product

inputstringph = ""; //clear the string:

input_stringcompleteph = false;//reset the flage used to tell if we have recived a completed string from the PC
```

```
}

while(mandar){

phserial.listen();

while (phserial.available()>0) { //while a char is holding in the serial buffer

char inchar = (char)phserial.read();//get the new char

sensorstringph += inchar; //add it to the sensorstringph

if (inchar == '\r') {sensor_stringcompleteph = true;} //if the incoming character is a <CR>, set the flag

}

if (sensor_stringcompleteph){ //if a string from the Atlas Scientific product has been received in its entirety

Serial.print(sensorstringph); //use the hardware serial port to send that data to the PC

sensorstringph = ""; //clear the string:

sensor_stringcompleteph = false; //reset the flag used to tell if we have received a completed string from the Atlas Scientific product

mandar=false;

}
}


// ******ORP*****

if (input_stringcompleteorp){ //if a string from the PC has been recived in its entierty

orpserial.print(inputstringorp); //send that string to the Atlas Scientific product

inputstringorp = ""; //clear the string:

input_stringcompleteorp = false;//reset the flage used to tell if we have recived a completed string from the PC

}

mandar=true;

while(mandar){
orpserial.listen();


while (orpserial.available()>0) { //while a char is holding in the serial buffer
```

```
char inchar = (char)orpserial.read();//get the new char

sensorstringorp += inchar; //add it to the sensorstringorp

if (inchar == '\r') {sensor_stringcompleteorp = true;} //if the incoming character is a <CR>, set the flag

}


// ******Analogic inputs*****
// ******THERMISTOR*****

int ntcext=analogRead(analogPin2); // leemos
// ******TERMISTOR SISTEMA*****

int ntcbiodig=analogRead(analogPin1); // leemos
//****print ****

int sensorpresion= analogRead(A0); // lee valor de presion

if (sensor_stringcompleteorp){//if a string from the Atlas Scientific product has been received in its entirety

Serial.print(sensorstringph);//use the hardware serial port to send that data to the PC

Serial.print(",");//use the hardware serial port to send that data to the PC

Serial.print(sensorstringorp);

Serial.print(",");

Serial.print(sensorpresion); // imprime valor de presion

Serial.print(",");

Serial.print(ntcext);

Serial.print(",");

Serial.println(ntcbiodig);

sensorstringorp = "";//clear the string:

sensor_stringcompleteorp = false;//reset the flag used to tell if we have received a completed string from the Atlas Scientific product

mandar=false;

}

}
}
```

Appendix C Processing Source Code

```
import processing.serial.*;
import controlP5.*;

String nom_archivo="name.txt";
String hora_inicio="Begining: "+hour()+":"+minute()+":"+second();
PrintWriter archivo;
ControlP5 cp5;
Serial myPort; // The serial port
boolean serialInited;
int xPos = 1; // horizontal position of the graph
int esquina_x=600;
int esquina_y=100;
int ancho=500;
int alto=300;
int pocision_alto=0;//posicion donde se colocan los datos en la grafica, menor que alto.
int guardar_datos=-1;
String dato_1="hola",dato_2="adios",dato_3="hasta",dato_4="luego",dato_5="vengo",
dato_6= "voy";
PShape bot;
int ancho_ventana=720,alto_ventana=400;
int x_r1=470,y_r1=100,dx_r1=200,dy_r1=230;
int mx_r1=10,my_r1=30,dy_t=30;
int x_r2=40,y_r2=100,dx_r2=385,dy_r2=130;
int mx_r2=10,my_r2=30;
int ancho_campo_texto=210;
int x_resto=40,y_resto=250,dy_resto=25;
int x_r3=40,y_r3=300,dx_r3=210,dy_r3=35;
int mx_r3=10,my_r3=30;
int ancho_boton=200,alto_boton=20;
int lf = 10; // Salto de linea en ASCII
int BAUD_RATE=9600;
String inString=null;



void setup () {

cp5 = new ControlP5(this);


cp5.addButton("Save_data")

.setValue(0)

.setPosition(x_resto,y_resto)

.setSize(ancho_boton,alto_boton)

;
```

```
cp5.addButton("Stop_save_data")

.setValue(0)

.setPosition(x_resto,y_resto+dy_resto)

.setSize(ancho_boton,alto_boton)

;


cp5.addTextfield("nom_archivo")

.setPosition(x_r2+mx_r2+ancho_campo_texto, y_r2+my_r2/3)

.setSize(150,25)

.setCaptionLabel("")

.setColorBackground(color(50,50,50))

.setColorActive(color(100,0,0))

.setColorForeground(color(100,0,0))

.setFont(createFont("arial",15))

;

//size(ancho_ventana,alto_ventana);
size(720,400);
stroke(127,0,0);
//rect(esquina_x, esquina_y, ancho, alto);

println(Serial.list());

myPort = new Serial(this, Serial.list()[0], 9600);//Se crea una comunicación serial en el
puerto 0, con 9600bd.
myPort.clear();
myPort.buffer(50);
inString = myPort.readStringUntil(lf);
inString = null;


background(0,255,200);

bot = loadShape("ULPGC.svg");
shape(bot, 20, 20, 70, 50);

String s_1="University of Las Palmas de Gran Canaria";
String s_2="Laboratory-scale biodigester.";
String s_3="Saved data";
```

```
String s_4="T= ";

textSize(20);
fill(0, 102, 153);
text(s_1, 95, 45);
text(s_2, 95, 65);
text(s_3, 95, 205);
fill(255, 255, 255);
}

void draw () {

//background(0,255,200);
fill(155, 255, 255);
rect(x_r1,y_r1,dx_r1,dy_r1);
color(250,0,0,205);
fill(0, 102, 153);
text("Measured variables", x_r1+mx_r1, y_r1+my_r1);
text("Tamb = "+dato_1+ "ºC", x_r1+mx_r1, y_r1+my_r1+dy_t);
text("Treact = "+dato_2+ "ºC", x_r1+mx_r1, y_r1+my_r1+2*dy_t);
text("P = "+dato_3+ " kPa", x_r1+mx_r1, y_r1+my_r1+3*dy_t);
text("ORP = "+dato_4+ " mV", x_r1+mx_r1, y_r1+my_r1+4*dy_t);
text("pH = "+dato_5, x_r1+mx_r1, y_r1+my_r1+5*dy_t);
text("Aux = "+dato_6, x_r1+mx_r1, y_r1+my_r1+6*dy_t);
fill(155, 255, 255);
rect(x_r2,y_r2,dx_r2,dy_r2);
//rect(40, 130, 385, 130);
color(250,0,0,205);
fill(0, 102, 153);
text("File name:",x_r2+mx_r2, y_r2+my_r2);
text(nom_archivo,x_r2+mx_r2, y_r2+my_r2+dy_t);
text(hora_inicio,x_r2+mx_r2, y_r2+my_r2+2*dy_t);
text("Saving: "+hour()+":"+minute()+":"+second(),x_r2+mx_r2, y_r2+my_r2+3*dy_t);
fill(255, 255, 255);
strokeWeight(1);
color(250,0,0,255);
strokeWeight(2);
fill(155, 255, 255);
rect(x_r3,y_r3,dx_r3,dy_r3);
color(250,0,0,205);
fill(0, 102, 153);

if(guardar_datos>0){
      color(255,255,0,0);
      fill(255, 0, 0);
      ellipse(x_r3+2*mx_r3, y_r3+my_r3/2, 15, 15);
      text("Saving",x_r3+4*mx_r3,y_r3+my_r3/1.25);
}
else{
      color(250,0,0,0);
      fill(0, 0, 0);
      ellipse(x_r3+2*mx_r3, y_r3+my_r3/2, 15, 15);
      text("Showing",x_r3+4*mx_r3,y_r3+my_r3/1.25);
}
```

```
}

void serialEvent (Serial myPort) {
// Toma una cadena de caracteres ASCII:
inString = myPort.readStringUntil('\n');
inString = trim(inString);

if (inString != null) {
      println(inString);
      String[] lista = split(inString,",");
      dato_1=lista[0];
      dato_2=lista[1];
      dato_3=lista[2];
      dato_4=lista[3];
      dato_5=lista[4];
      dato_6="—";//lista[5];


if(guardar_datos>0){
      archivo.print(month( )+" ");
      archivo.print(day( )+" ");
      archivo.print(year( )+" ");
      archivo.print(hour( )+" ");
      archivo.print(minute( )+" ");
      archivo.print(second( )+" ");
      archivo.print(dato_1+" ");
      archivo.print(dato_2+" ");
      archivo.print(dato_3+" ");
      archivo.print(dato_4+" ");
      archivo.print(dato_5+" ");
      archivo.println(dato_6+" ");
      archivo.flush(); // Writes the remaining data to the file
}
}
}

public void Save_data(int theValue) {

println("a button event from colorA: "+theValue);

//++dato_prueba;

archivo = createWriter(nom_archivo);

hora_inicio="Begining: "+hour()+":"+minute()+":"+second();

if(guardar_datos>0){int r=0;}

else{

guardar_datos=-1*guardar_datos;

}
}
```

```
public void Stop_save_data(int theValue) {

println("a button event from colorA: "+theValue);

//++dato_prueba;

guardar_datos=-1;

archivo.flush(); // Writes the remaining data to the file

archivo.close(); // Finishes the file

nom_archivo="name.txt";
}
```

References

1. Brito-Espino, S.; Ramos-Martín, A.; Pérez-Báez, S.O.; Mendieta-Pino, C.; Leon-Zerpa, F. A Framework Based on Finite Element Method (FEM) for Modelling and Assessing the Affection of the Local Thermal Weather Factors on the Performance of Anaerobic Lagoons for the Natural Treatment of Swine Wastewater. *Water* **2021**, *13*, 882. [CrossRef]
2. Cano, E.; Ruiz, J.G.; Garcia, I.A. Integrating a learning constructionist environment and the instructional design approach into the definition of a basic course for embedded systems design. *Comput. Appl. Eng. Educ.* **2015**, *23*, 36–53. [CrossRef]
3. Garcia, I.A.; Cano, E.M. Designing and implementing a constructionist approach for improving the teaching-learning process in the embedded systems and wireless communications areas. *Comput. Appl. Eng. Educ.* **2014**, *22*, 481–493. [CrossRef]
4. Available online: http://www.atago.net/Spanish/download.htmlRX-7000i (accessed on 11 June 2021).
5. Refractómetro Digital Automático Atago. Available online: http://www.atago.net/Spanish/download.html (accessed on 14 June 2021).
6. Jagnow, G.; Dawind, W. *Biotecnología: Introducción Con Experimentos Modelo*; Acribia S.A.: Zaragoza, Spain, 1991.
7. Liu, C.-G.; Xue, C.; Lin, Y.-H.; Bai, F.-W. Redox potential control and applications in microaerobic and anaerobic fermentations. *Biotechnol. Adv.* **2013**, *31*, 257–265. [CrossRef]
8. Madsen, M.; Holm-Nielsen, J.B.; Esbensen, K.H. Monitoring of anaerobic digestion processes: A review perspective. *Renew. Sustain. Energy Rev.* **2011**, *15*, 3141–3155. [CrossRef]
9. Mekic, E.; Djokic, I.; Zejnelagic, S.; Matovic, A. Constructive approach in teaching of voip in line with good laboratory and manufacturing practice. *Comput. Appl. Eng. Educ.* **2016**, *24*, 277–287. [CrossRef]
10. Pantaleo, A.; De Gennaro, B.; Shah, N. Assessment of optimal size of anaerobic co- digestion plants: An application to cattle farms in the province of bari (Italy). *Renew. Sustain. Energy Rev.* **2013**, *20*, 57–70. [CrossRef]
11. Atlas Scientific. Atlas Scientific. Orpatlas. Available online: https://atlas-scientific.com/?gclid=EAIaIQobChMIvbPk8o3Z8gIVied3Ch03AgqaEAAYASAAEgKLzPD_BwE (accessed on 19 July 2021).
12. Sorathia, K.; Servidio, R. Learning and experience: Teaching tangible interaction & edutainment. *Procedia—Soc. Behav. Sci.* **2012**, *64*, 265–274.
13. Taylhardat Arjona, L.A. *El biogas. Fundamentos e Infraestructura Rural*; Instituto de Ingenieria Agri- cola; Facultad de Agronomia U.C.V: Maracay, Venezuela, 1986.
14. Leon, F.; Ramos, A.; Vaswani, J.; Mendieta, C.; Brito, S. Climate Change Mitigation Strategy through Membranes Replacement and Determination Methodology of Carbon Footprint in Reverse Osmosis RO Desalination Plants for Islands and Isolated Territories. *Water* **2021**, *13*, 293. [CrossRef]
15. Products for USB Sensing and Control. Products for Usb Sensing and Control. Available online: www.phidgets.com (accessed on 1 July 2021).
16. Parralejo, A.; Royano, L.; González, J.; González, J. Small scale biogas production with animal excrement and agricultural residues. *Ind. Crops Prod.* **2019**, *131*, 307–314. [CrossRef]
17. Holm-Nielsen, J.; Seadi, T.A.; Oleskowicz-Popiel, P. The future of anaerobic digestion and biogas utilization. *Bioresour. Technol.* **2009**, *100*, 5478–5484. [CrossRef]
18. Park, J.H.; Park, J.H.; Lee, S.H.; Jung, S.P.; Kim, S.H. Enhancing anaerobic digestion for rural wastewater treatment with granular activated carbon (GAC) supplementation. *Bioresour. Technol.* **2020**, *315*, 123890. [CrossRef] [PubMed]
19. Jiang, Y.; Bebee, B.; Mendoza, A.; Robinson, A.K.; Zhang, X.; Rosso, D. Energy footprint and carbon emission reduction using off-the-grid solar-powered mixing for lagoon treatment. *J. Environ. Manag.* **2018**, *205*, 125–133. [CrossRef] [PubMed]
20. Duan, N.; Zhang, D.; Khoshnevisan, B.; Kougias, P.G.; Treu, L.; Liu, Z.; Lin, C.; Liu, H.; Zhang, Y.; Angelidaki, I. Human waste anaerobic digestion as a promising low-carbon strategy: Operating performance, microbial dynamics and environmental footprint. *J. Clean. Prod.* **2020**, *256*, 120414. [CrossRef]

21. Mendieta-Pino, C.A.; Ramos-Martin, A.; Perez-Baez, S.O.; Brito-Espino, S. Management of slurry in Gran Canaria Island with full-scale natural treatment systems for wastewater (NTSW). One year experience in livestock farms. *J. Environ. Manag.* **2019**, *232*, 666–678.
22. Muga, H.; Mihelcic, J. Sustainability of wastewater treatment technologies. *J. Environ. Manag.* **2008**, *88*, 437–447. [CrossRef]
23. Wu, B.; Chen, Z. An integrated physical and biological model for anaerobic lagoons. *Bioresour. Technol.* **2011**, *102*, 5032–5038. [CrossRef] [PubMed]
24. Wu, B. Advances in the use of CFD to characterize, design and optimize bioenergy systems. *Comput. Electron. Agric.* **2013**, *93*, 195–208. [CrossRef]
25. Donoso-Bravo, A.; Sadino-Riquelme, C.; Gómez, D.; Segura, C.; Valdebenito, E.; Hansen, F. Modelling of an anaerobic plug-flow reactor. Process analysis and evaluation approaches with non-ideal mixing considerations. *Bioresour. Technol.* **2018**, *260*, 95–104.
26. Rajeshwari, K.; Balakrishnan, M.; Kansal, A.; Lata, K.; Kishore, V. State-of-the-art of anaerobic digestion technology for industrial wastewater treatment. *Renew. Sustain. Energy Rev.* **2000**, *4*, 135–156. [CrossRef]
27. Lauwers, J.; Appels, L.; Thompson, I.P.; Degrève, J.; Impe, J.F.V.; Dewil, R. Mathematical modelling of anaerobic digestion of biomass and waste: Power and limitations. *Prog. Energy Combust.* **2013**, *39*, 383–402. [CrossRef]
28. Wade, M.; Harmand, J.; Benyahia, B.; Bouchez, T.; Chaillou, S.; Cloez, B. Perspectives in mathematical modelling for microbial ecology. *Ecol. Model.* **2016**, *321*, 64–74. [CrossRef]
29. Batstone, D.; Keller, J.; Angelidaki, I.; Kalyuzhnyi, S.; Pavlostathis, S.; Rozzi, A.; Sanders, W.; Siegrist, H.; Vavilin, V. The IWAAnaerobic Digestion Model No 1 (ADM1). *Water Sci. Technol.* **2002**, *45*, 65–73. Available online: https://library.lanl.gov/cgi-bin/getfile?00285556.pdf (accessed on 1 September 2020). [CrossRef]
30. Kleerebezem, R.; van Loosdrecht, M.C.M. Critical analysis of some concepts proposed in ADM1. *Water Sci. Technol.* **2006**, *54*, 51–57. [CrossRef] [PubMed]
31. Li, D.; Lee, I.; Kim, H. Application of the linearized ADM1 (LADM) to lab-scale anaerobic digestion system. *J. Environ. Chem. Eng.* **2021**, *9*, 105193. [CrossRef]
32. Fleming, J.G. Novel Simulation of Anaerobic Digestion Using Computational Fluid Dynamics. Ph.D. Thesis, North Carolina State University, Raleigh, NC, USA, 2002.
33. Goodarzi, D.; Sookhak Lari, K.; Mossaiby, F. Thermal effects on the hydraulic performance of sedimentation ponds. *J. Water Process. Eng.* **2020**, *33*, 101100. [CrossRef]
34. Brito-Espino, S.; Ramos-Martín, A.; Pérez-Báez, S.; Mendieta-Pino, C. Application of a mathematical model to predict simultaneous reactions in anaerobic plug-flow reactors as a primary treatment for constructed wetlands. *Sci. Total Environ.* **2020**, *713*, 136244. [CrossRef]
35. Mahmudul, H.; Rasul, M.; Akbar, D.; Narayanan, R.; Mofijur, M. A comprehensive review of the recent development and challenges of a solar-assisted biodigester system. *Sci. Total Environ.* **2021**, *753*, 141920. [CrossRef] [PubMed]
36. Atelge, M.; Atabani, A.; Banu, J.R.; Krisa, D.; Kaya, M.; Eskicioglu, C.; Kumar, G.; Lee, C.; Yildiz, Y.; Unalan, S.; et al. A critical review of pretreatment technologies to enhance anaerobic digestion and energy recovery. *Fuel* **2020**, *270*, 117494. [CrossRef]
37. Tumilar, A.S.; Milani, D.; Cohn, Z.; Florin, N.; Abbas, A. A Modelling Framework for the Conceptual Design of Low-Emission Eco-Industrial Parks in the Circular Economy: A Case for Algae-Centered Business Consortia. *Water* **2021**, *13*, 69. [CrossRef]
38. Haßler, S.; Ranno, A.M.; Behr, M. Finite-element formulation for advection–reaction equations with change of variable and discontinuity capturing. *Comput. Methods Appl. Mech. Eng.* **2020**, *369*, 113171. [CrossRef]
39. Mirza, I.A.; Akram, M.S.; Shah, N.A.; Imtiaz, W.; Chung, J.D. Analytical solutions to the advection-diffusion equation with Atangana-Baleanu time-fractional derivative and a concentrated loading. *Alex. Eng. J.* **2021**, *60*, 1199–1208. [CrossRef]
40. Singh, S.; Bansal, D.; Kaur, G.; Sircar, S. Implicit-explicit-compact methods for advection diffusion reaction equations. *Comput. Fluids* **2020**, *212*, 104709. [CrossRef]
41. Zeng, L.; Chen, G. Ecological degradation and hydraulic dispersion of contaminant in wetland. *Ecol. Model.* **2011**, *222*, 293–300. [CrossRef]
42. Bozkurt, S.; Moreno, L.; Neretnieks, I. Long-term processes in waste deposits. *Sci. Total Environ.* **2000**, *250*, 101–121. [CrossRef]
43. Song, L.; Li, P.W.; Gu, Y.; Fan, C.M. Generalized finite difference method for solving stationary 2D and 3D Stokes equations with a mixed boundary condition. *Comput. Math. Appl.* **2020**, *80*, 1726–1743. [CrossRef]
44. Ukai, S. A solution formula for the Stokes equation in Rn+. *Commun. Pure Appl. Math.* **1987**, *40*, 611–621. [CrossRef]
45. Reddy, J.; Gartling, D. *The Finite Element Method in Heat Transfer and Fluid Dynamics*, 3rd ed.; CRC Press: Boca Raton, FL, USA, 2010; pp. 1–483.
46. Alvarez-Hostos, J.C.; Bencomo, A.D.; Puchi-Cabrera, E.S.; Fachinotti, V.D.; Tourn, B.; Salazar-Bove, J.C. Implementation of a standard stream-upwind stabilization scheme in the element-free Galerkin based solution of advection-dominated heat transfer problems during solidification in direct chill casting processes. *Eng. Anal. Bound. Elem.* **2019**, *106*, 170–181. [CrossRef]
47. Guldentops, G.; Van Dessel, S. A numerical and experimental study of a cellular passive solar façade system for building thermal control. *Sol. Energy* **2017**, *149*, 102–113. [CrossRef]
48. Lawrence, M.G. The Relationship between Relative Humidity and the Dewpoint Temperature in Moist Air: A Simple Conversion and Applications. *Bull. Am. Meteorol. Soc.* **2005**, *86*, 225–234. [CrossRef]
49. Çengel, Y. Heat Transfer: A Practical Approach. In *McGraw-Hill Series in Mechanical Engineering*; McGraw Hill Books: London, UK, 2003.

50. Walton, G.N. *Thermal Analysis Research Program Reference Manual*; NBSIR, Department of Energy, Office of Building Energy Research and Development: Washington, DC, USA, 1983.
51. Monod, J. The Growth of Bacterial Cultures. *Annu. Rev. Microbiol.* **1949**, *3*, 371–394. [CrossRef]
52. Rosso, L.; Lobry, J.; Flandrois, J. An Unexpected Correlation between Cardinal Temperatures of Microbial Growth Highlighted by a New Model. *J. Theor. Biol.* **1993**, *162*, 447–463. [CrossRef] [PubMed]
53. Herus, V.A.; Ivanchuk, N.V.; Martyniuk, P.M. A System Approach to Mathematical and Computer Modeling of Geomigration Processes Using Freefem++ and Parallelization of Computations. *Cybern Syst. Anal.* **2018**, *54*, 284–292. [CrossRef]
54. Donoso-Bravo, A.; Bandara, W.; Satoh, H.; Ruiz-Filippi, G. Explicit temperature-based model for anaerobic digestion: Application in domestic wastewater treatment in a UASB reactor. *Bioresour. Technol.* **2013**, *133*, 437–442. [CrossRef]
55. Donoso-Bravo, A.; Retamal, C.; Carballa, M.; Ruiz-Filippi, G.; Chamy, R. Influence of temperature on the hydrolysis, acidogenesis and methanogenesis in mesophilic anaerobic digestion: Parameter identification and modeling application. *Water Sci. Technol.* **2009**, *60*, 9–17. [CrossRef]
56. Wang, R.; Lv, N.; Li, C.; Cai, G.; Pan, X.; Li, Y.; Zhu, G. Novel strategy for enhancing acetic and formic acids generation in acidogenesis of anaerobic digestion via targeted adjusting environmental niches. *Water Res.* **2021**, *193*, 116896. Available online: https://www.sciencedirect.com/science/article/pii/S0043135421000944 (accessed on 23 June 2021). [CrossRef]
57. Weißbach, M.; Drewes, J.E.; Koch, K. Application of the oxidation reduction potential (ORP) for process control and monitoring nitrite in a Coupled Aerobic-anoxic Nitrous Decomposition Operation (CANDO). *Chem. Eng. J.* **2018**, *343*, 484–491. Available online: https://www.sciencedirect.com/science/article/pii/S1385894718303929 (accessed on 30 June 2021). [CrossRef]
58. Ao, T.; Chen, L.; Zhou, P.; Liu, X.; Li, D. The role of oxidation-reduction potential as an early warning indicator, and a microbial instability mechanism in a pilot-scale anaerobic mesophilic digestion of chicken manure. *Renew. Energy* **2021**, *179*, 223–232. Available online: https://www.sciencedirect.com/science/article/pii/S0960148121010521 (accessed on 1 July 2021). [CrossRef]